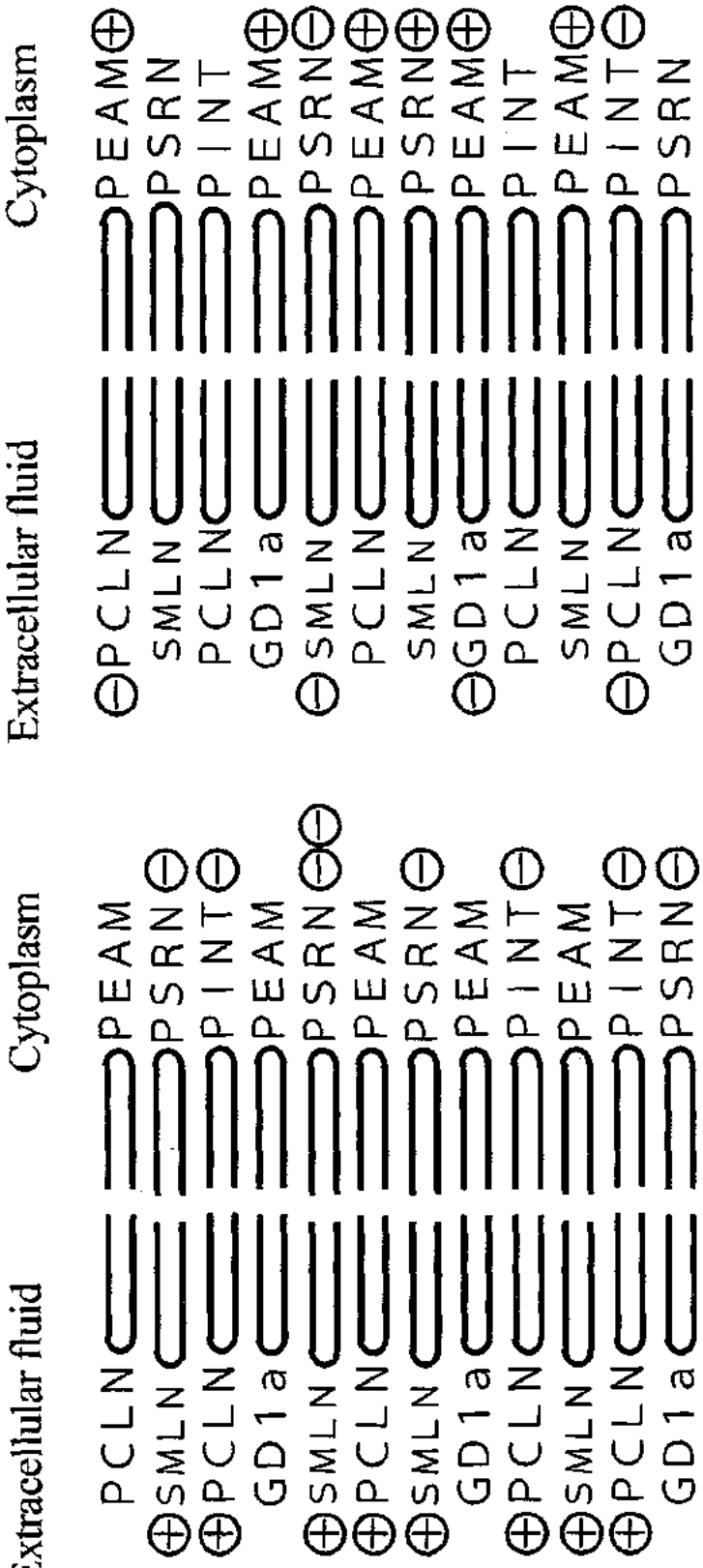



(a) In case of resting potential (b) In case of action potential

FIG.1 Charging model on both surfaces of neuronal membrane in case of action and resting potentials
PCLN : Phosphatidylcholine, SMLN : Sphingomyelin, GD1a : Ganglioside type D1a,
PSRN : Phosphatidylserine, PEAM : Phosphatidylethanolamine, PINT : Phosphatidylinositol.

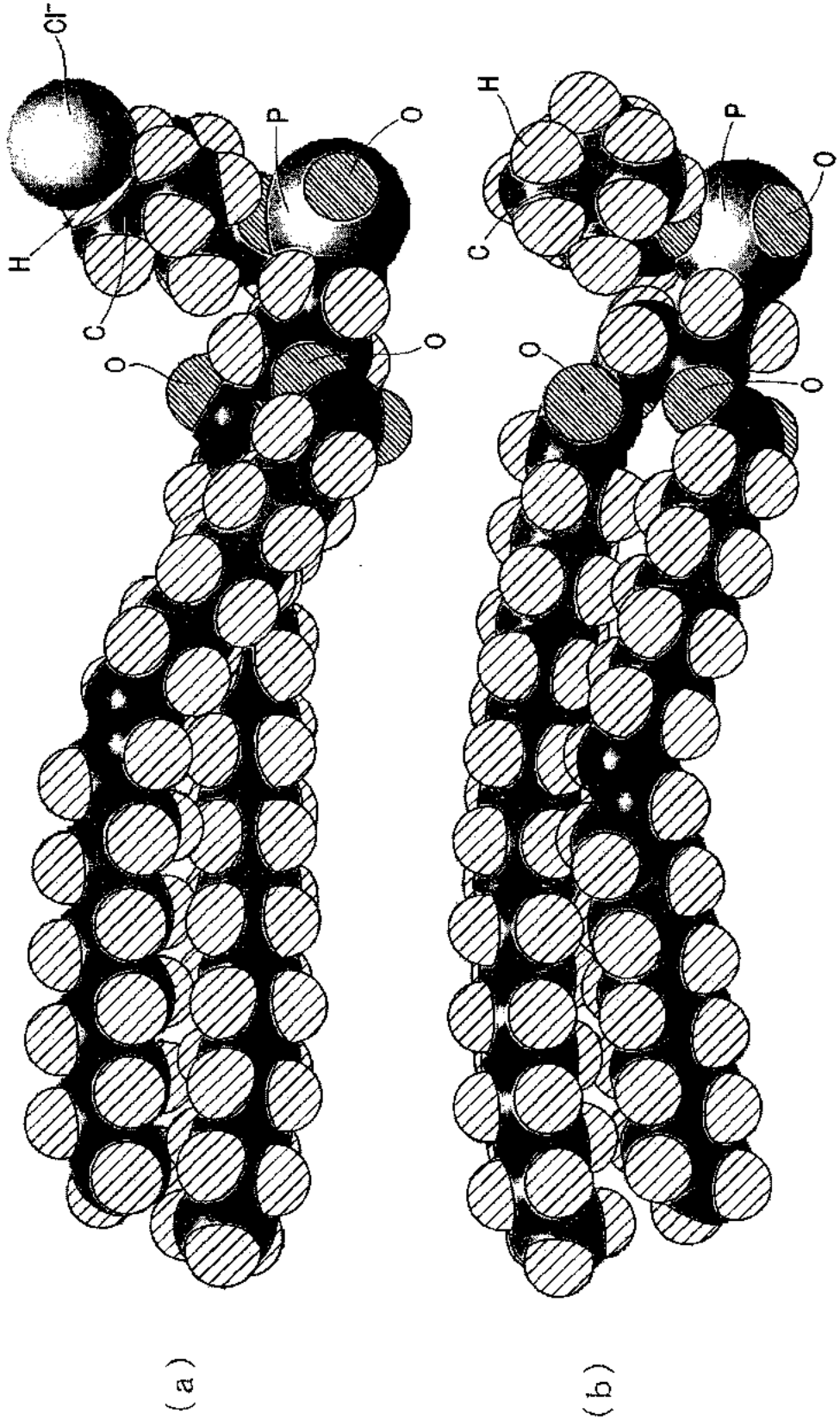



FIG. 2 Estimated molecular structure of PCLN in case of $Cl^-$ ion attachment and detachment

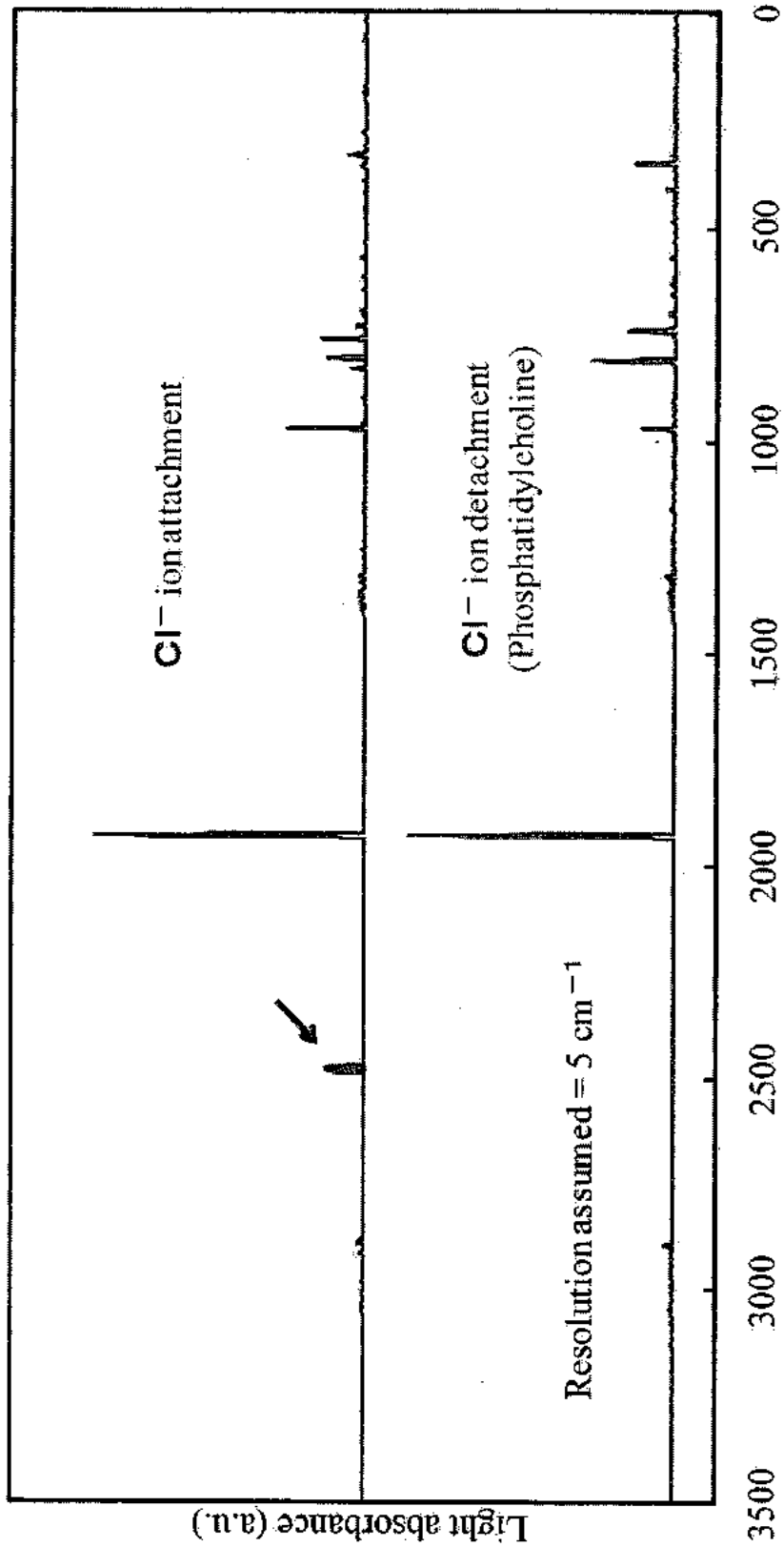



FIG. 3 Infrared spectral characteristics estimation of PCLN in case of Cl⁻ ion attachment and detachment.

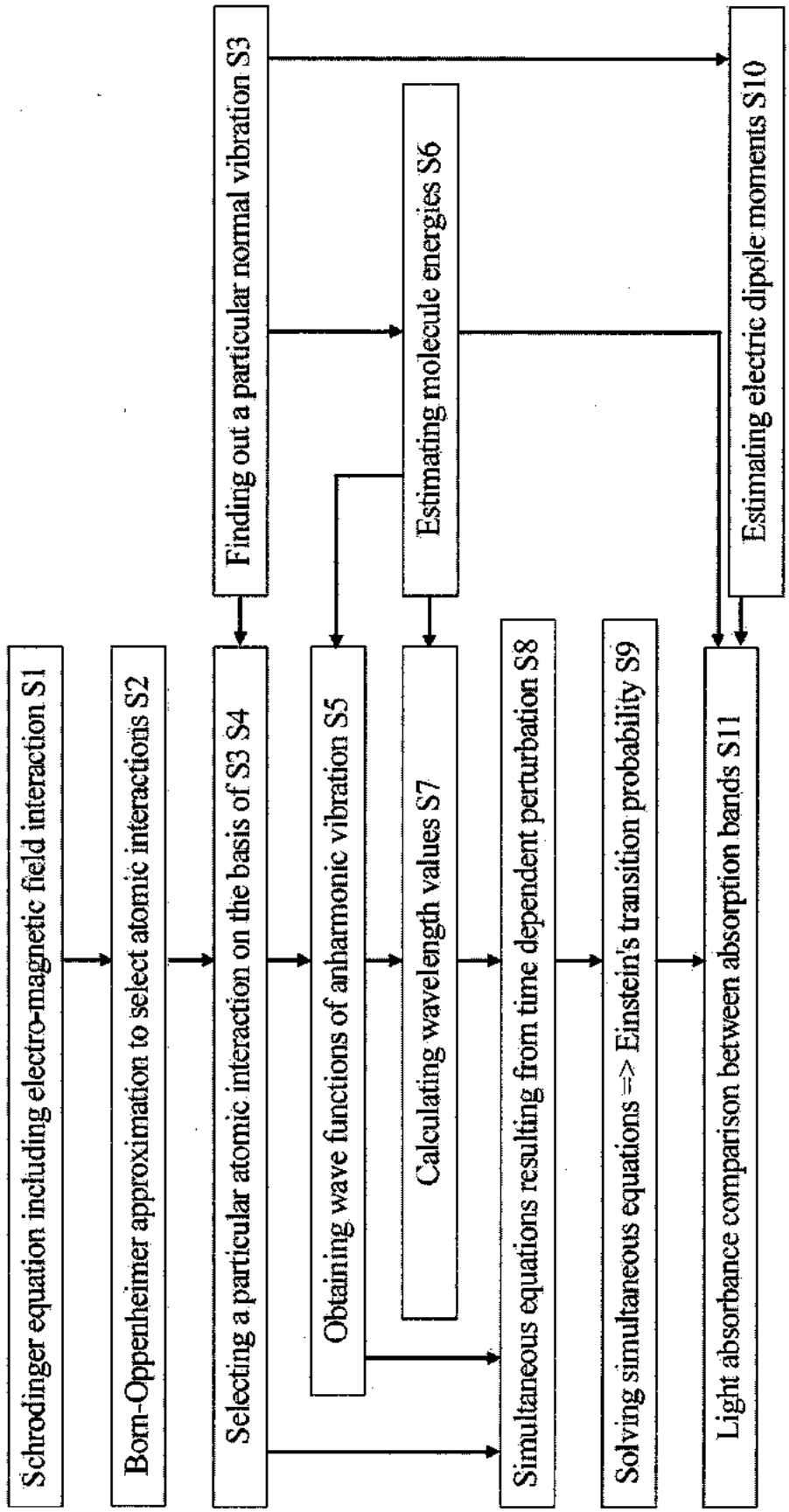



FIG .4 Flow chart used for originally calculating near infrared spectral characteristics based on anharmonic vibrations

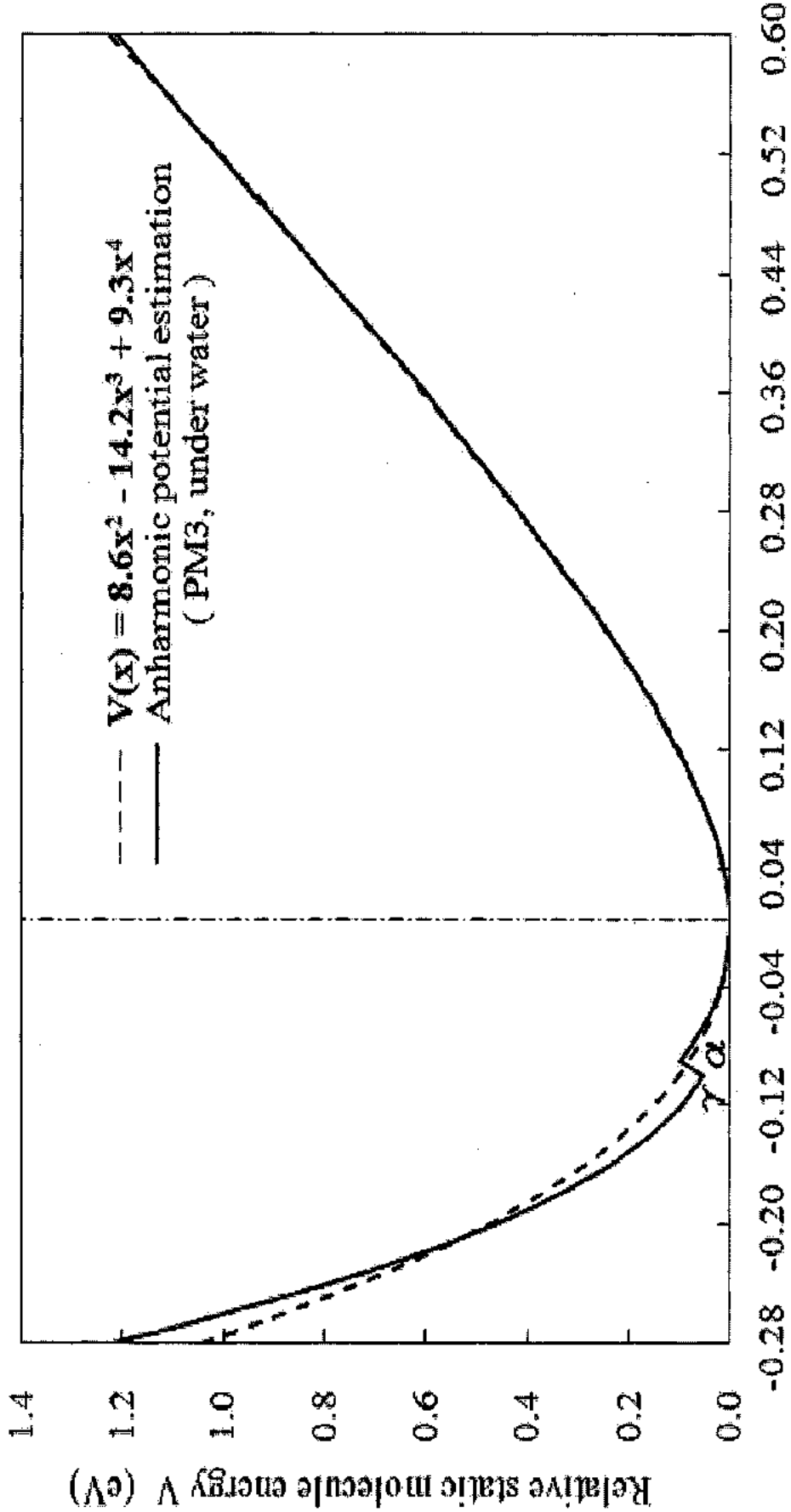



FIG.5 Relative static molecule energy vs. distance deviation between carbon and hydrogen atomic nucleuses.

(a) Atomic arrangement when the distance between carbon and hydrogen atomic nucleuses is appropriate

(b) Atomic arrangement when the distance between carbon and hydrogen atomic nucleuses is 0.10 (A) smaller than the appropriate value

FIG. 6. Cl⁻potision fluctuation dependent on distance deviation of carbon and hydrogen atomic nucleuses.

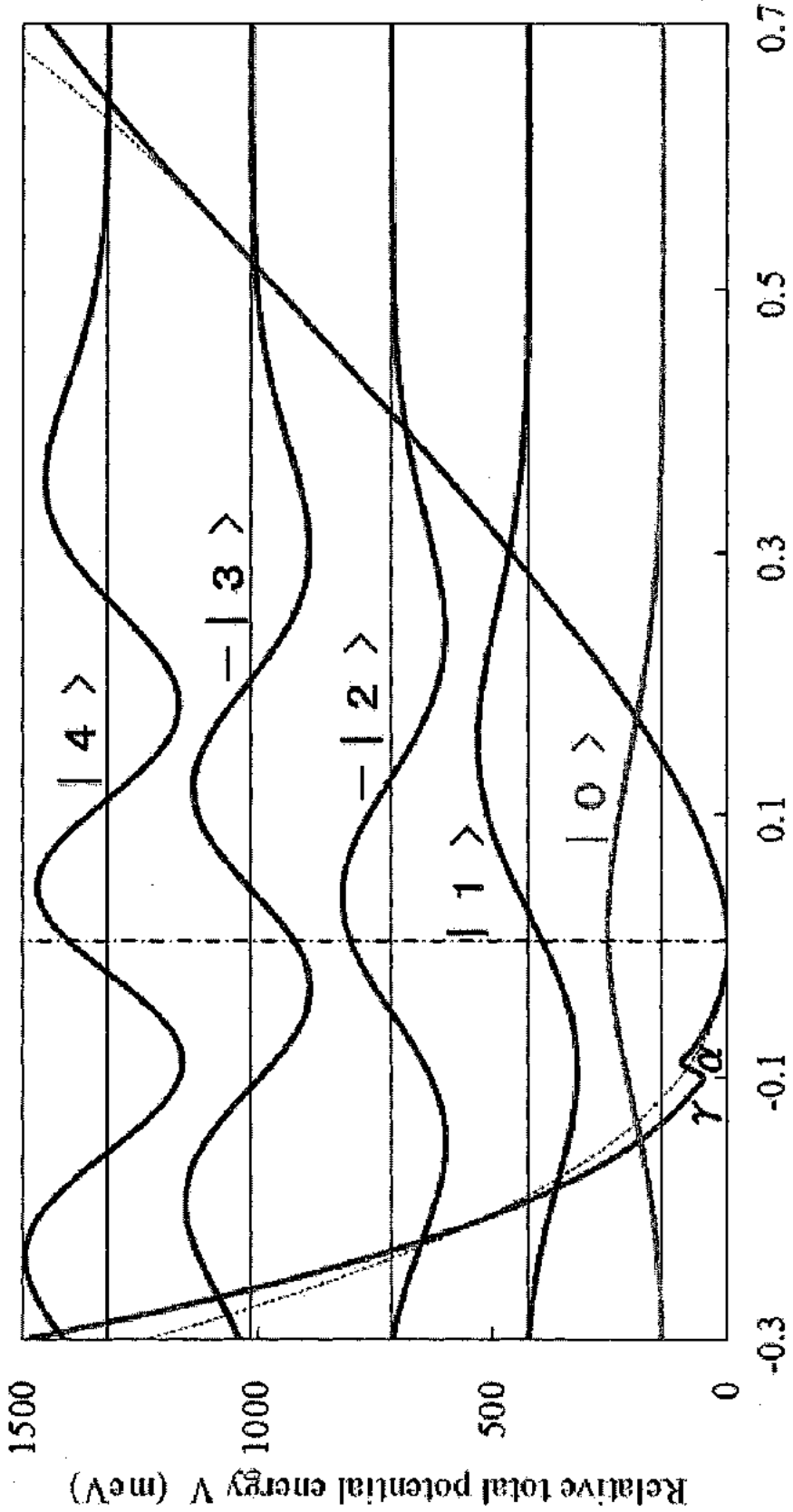



FIG . 7 Amplitude distributions of wave functions | m > regarding anharmonic vibrations.

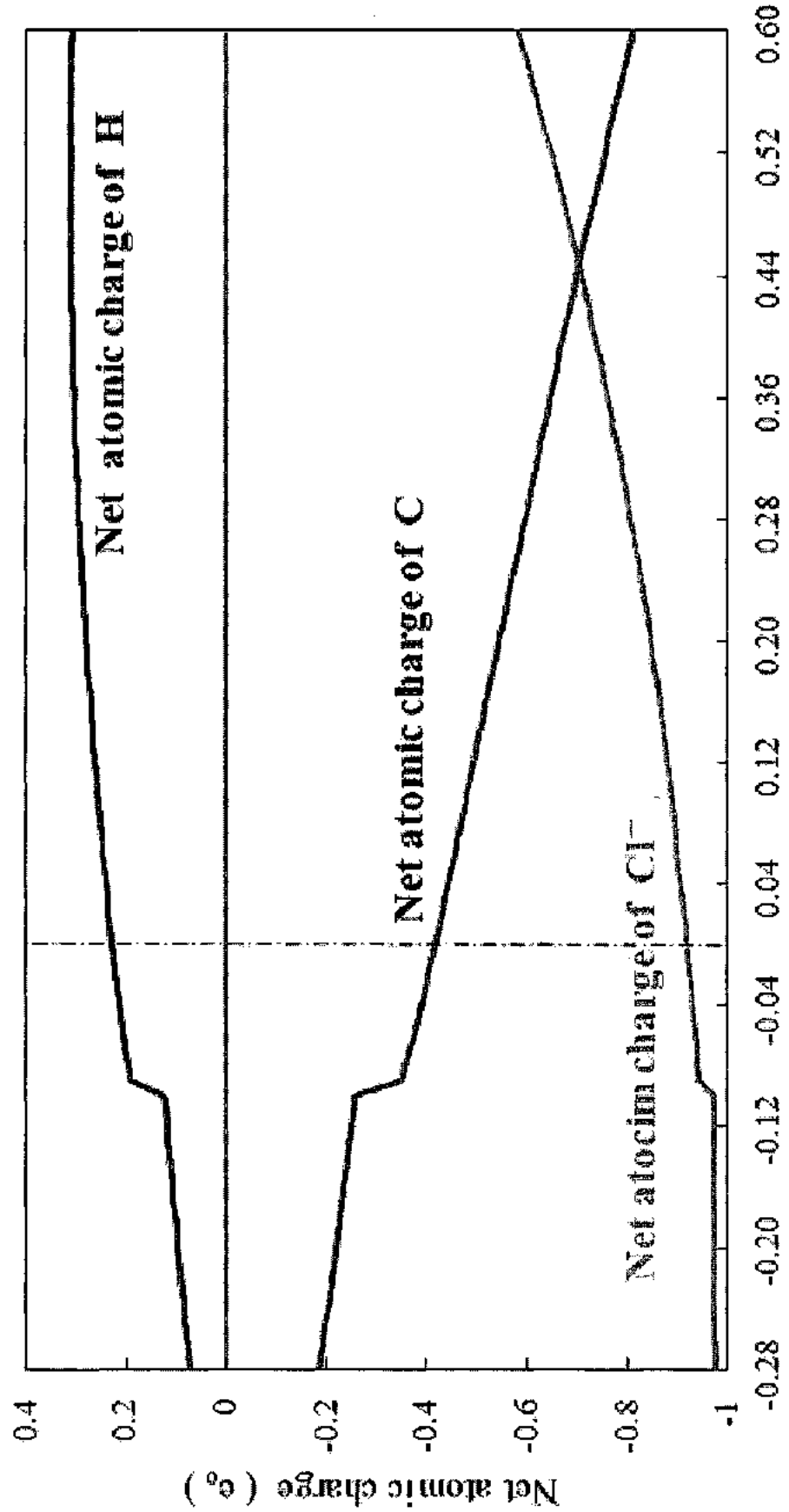
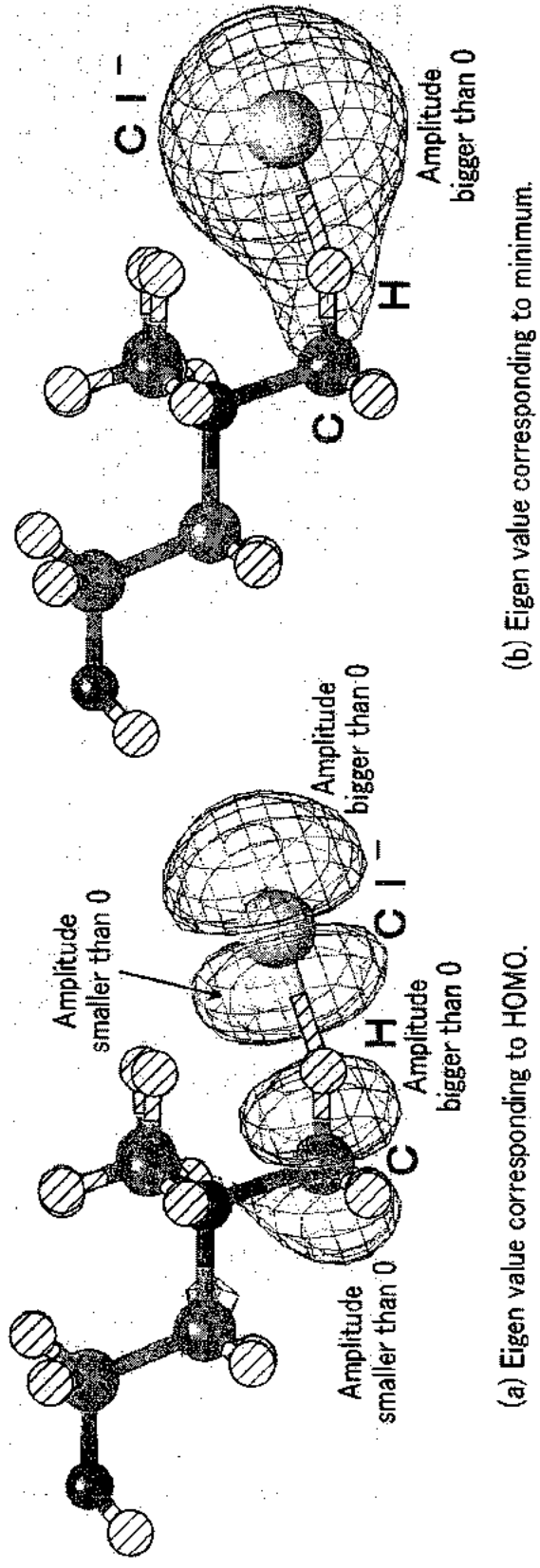



FIG. 8 Net atomic charges vs. distance deviations between carbon and hydrogen atomic nucleuses




(a) Eigen value corresponding to HOMO. (b) Eigen value corresponding to minimum.

FIG.9 Amplitude distributions of molecular orbitals whose eigen values of energy correspond to HOMO and the minimum

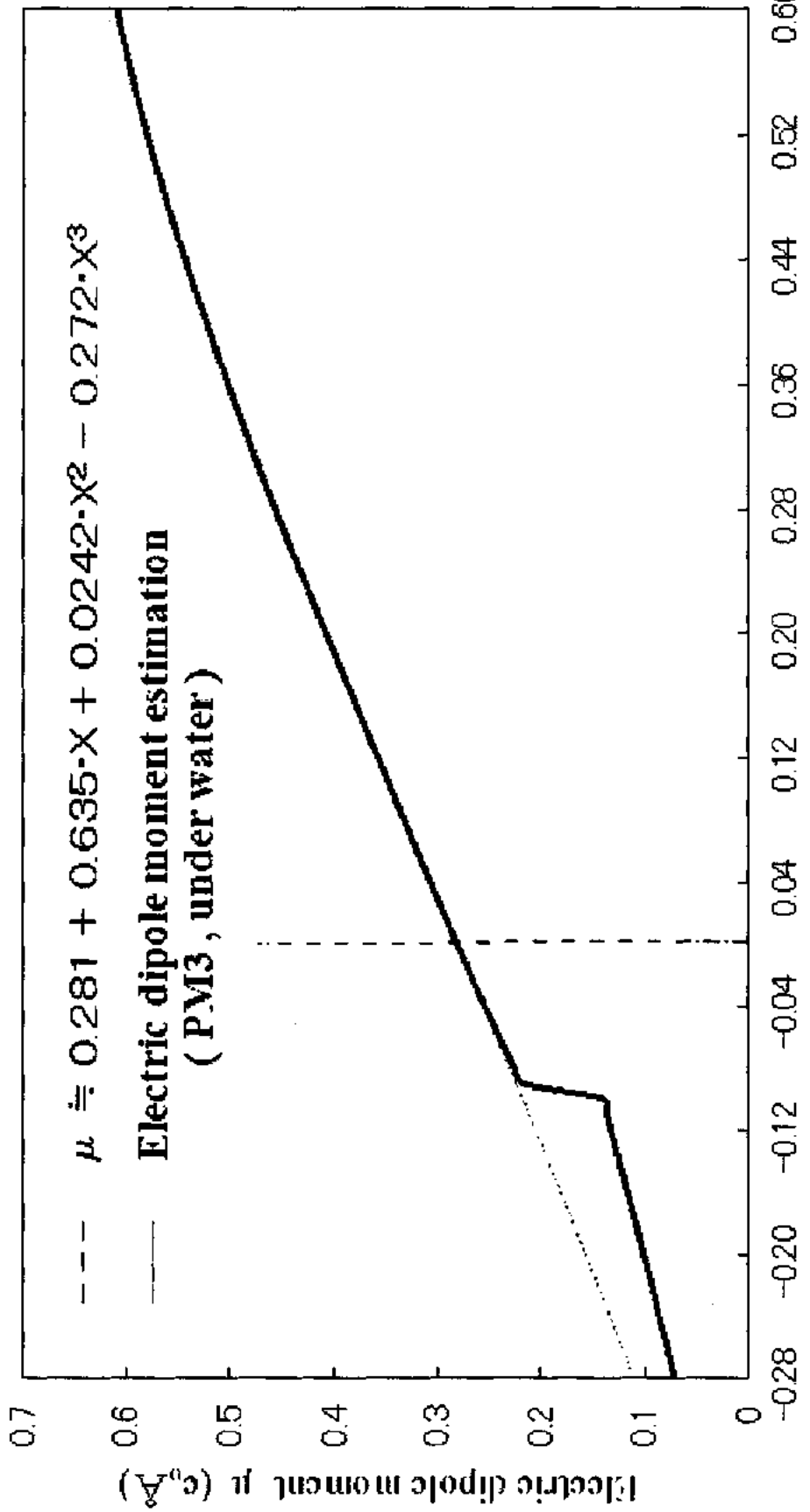



FIG .10 Electric dipole moments vs. distance deviations between carbon and hydrogen atomic nucleuses

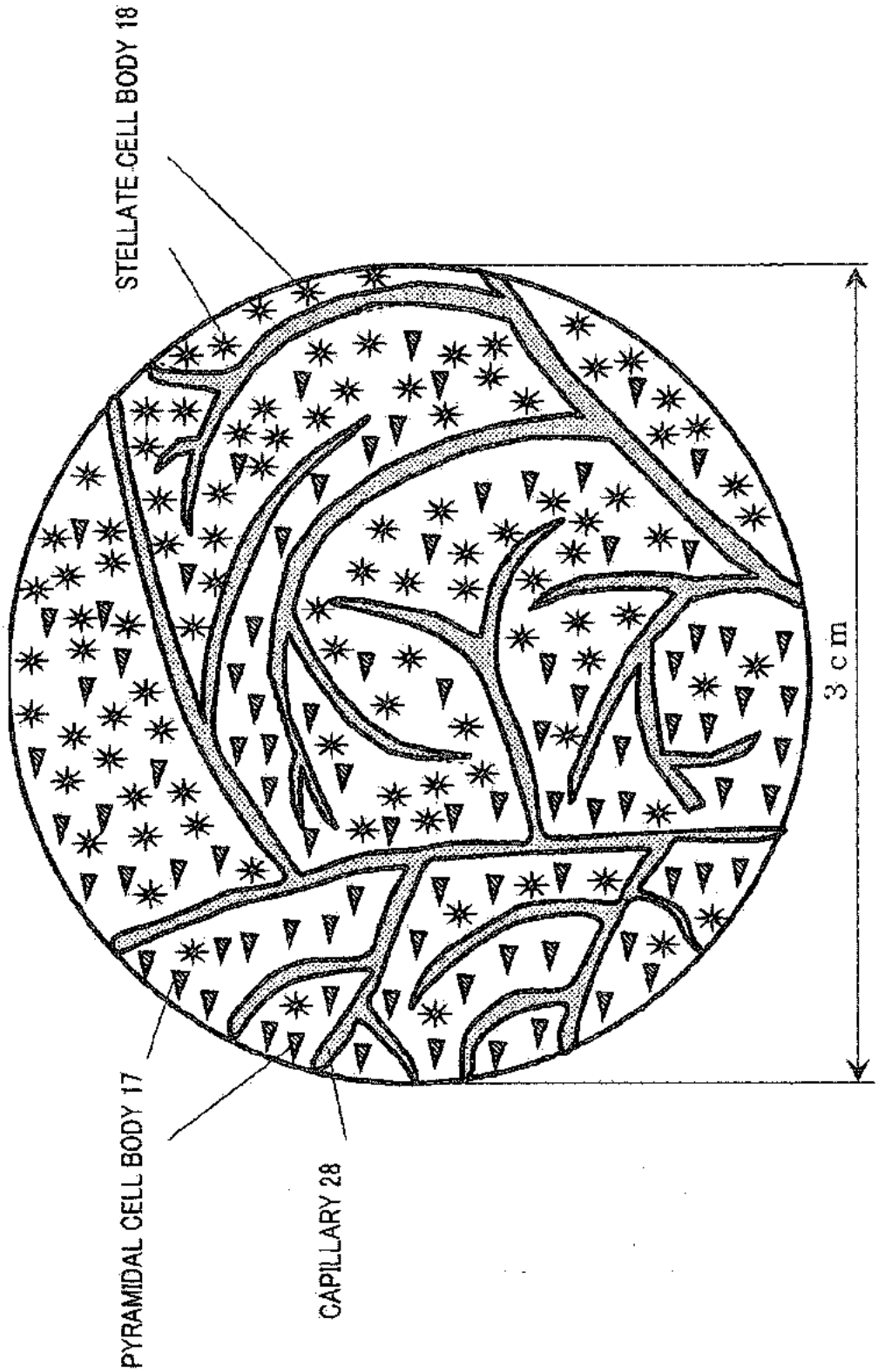



FIG.11 COMPARISON IN SPATIAL RESOLUTION BETWEEN MEMBRANE POTENTIAL CHANGING DETECTION AND OXYGEN CONCENTRATION CHANGE DETECTION IN BLOOD

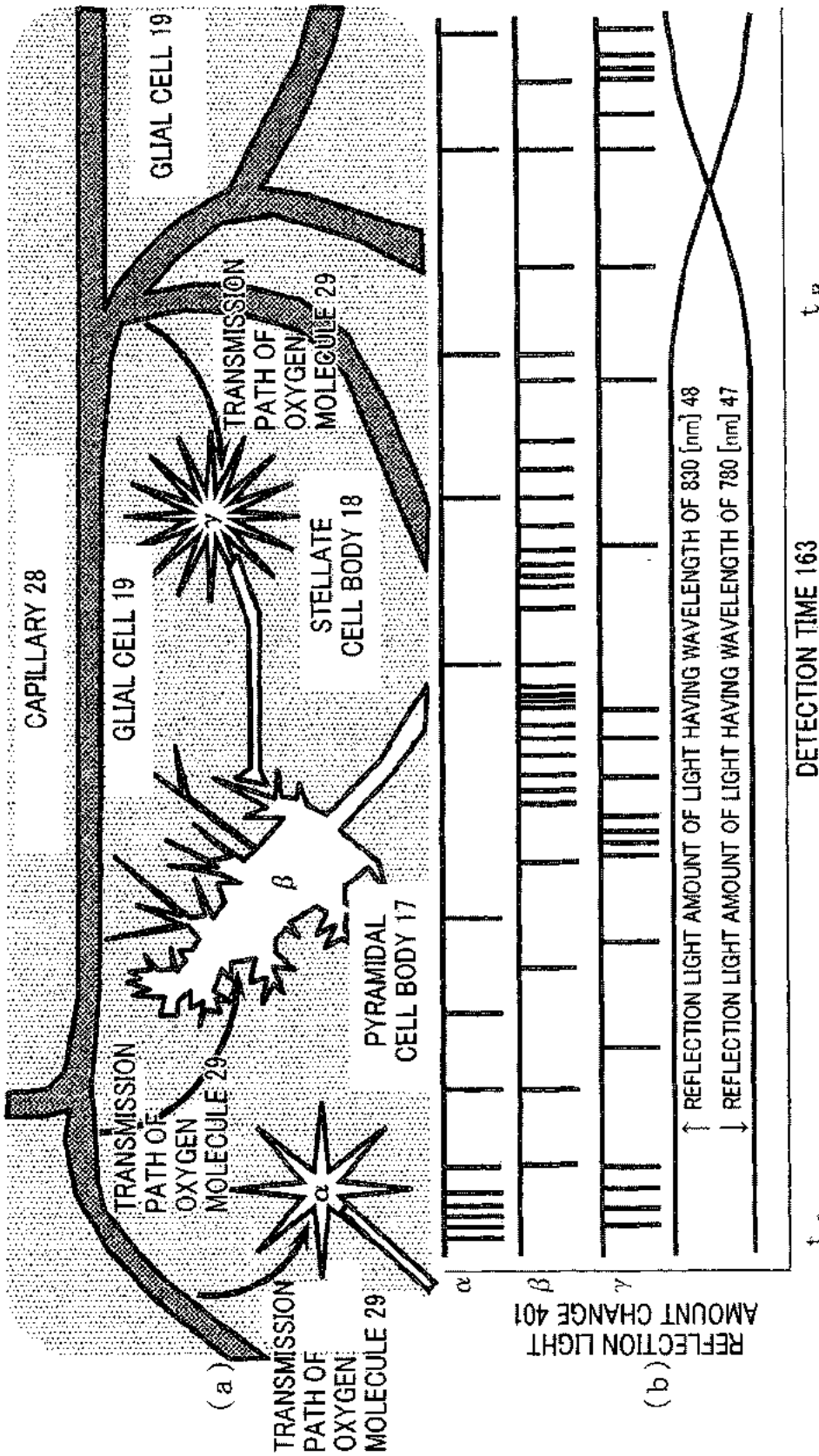



FIG.12 COMPARISON IN TEMPORAL RESOLUTION BETWEEN MEMBRANE POTENTIAL CHANGING DETECTION AND OXYGEN CONCENTRATION CHANGE DETECTION IN BLOOD

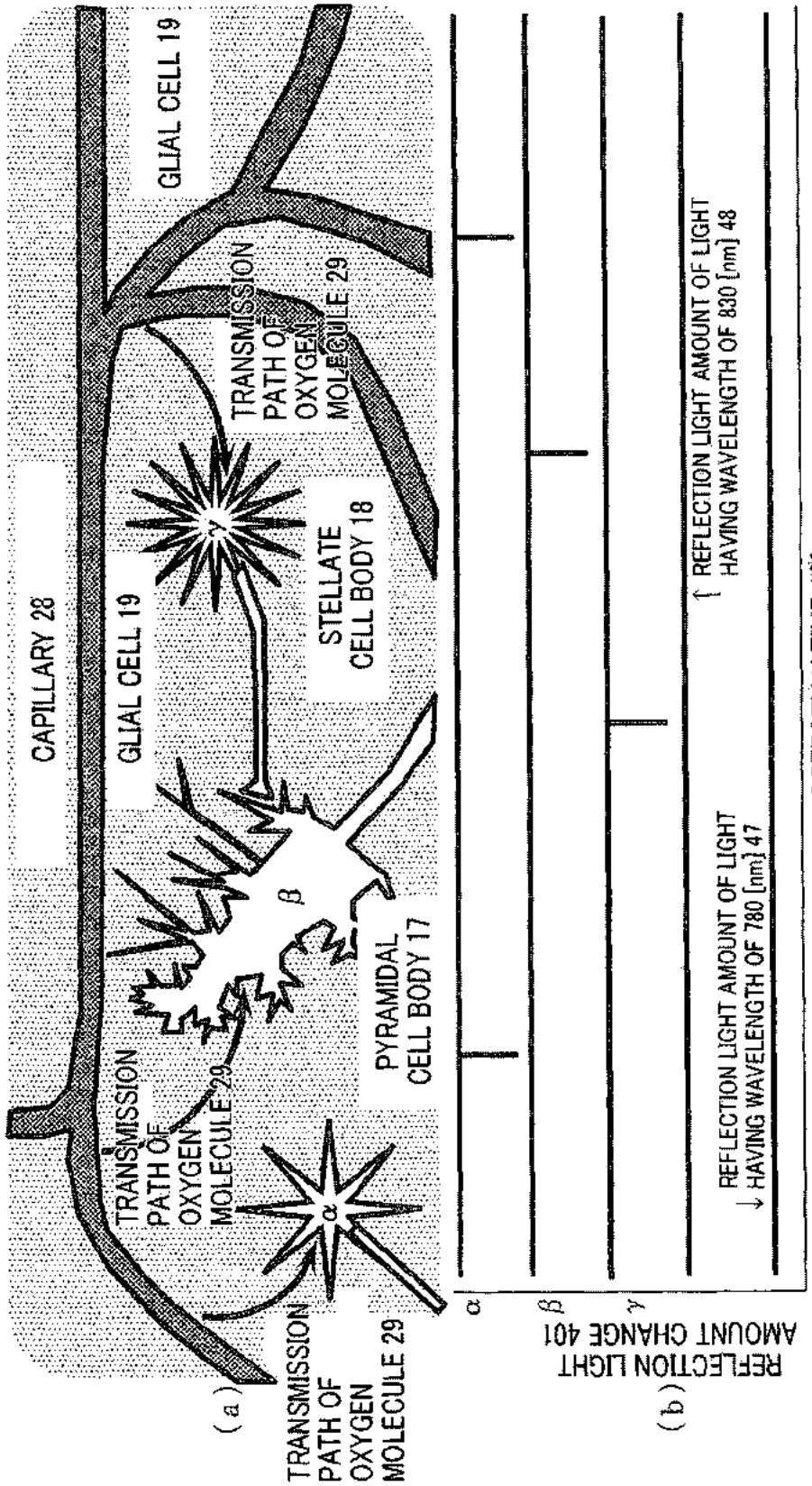



FIG.13 COMPARISON IN DETECTION ACCURACY BETWEEN MEMBRANE POTENTIAL CHANGING DETECTION AND OXYGEN CONCENTRATION CHANGE DETECTION IN BLOOD

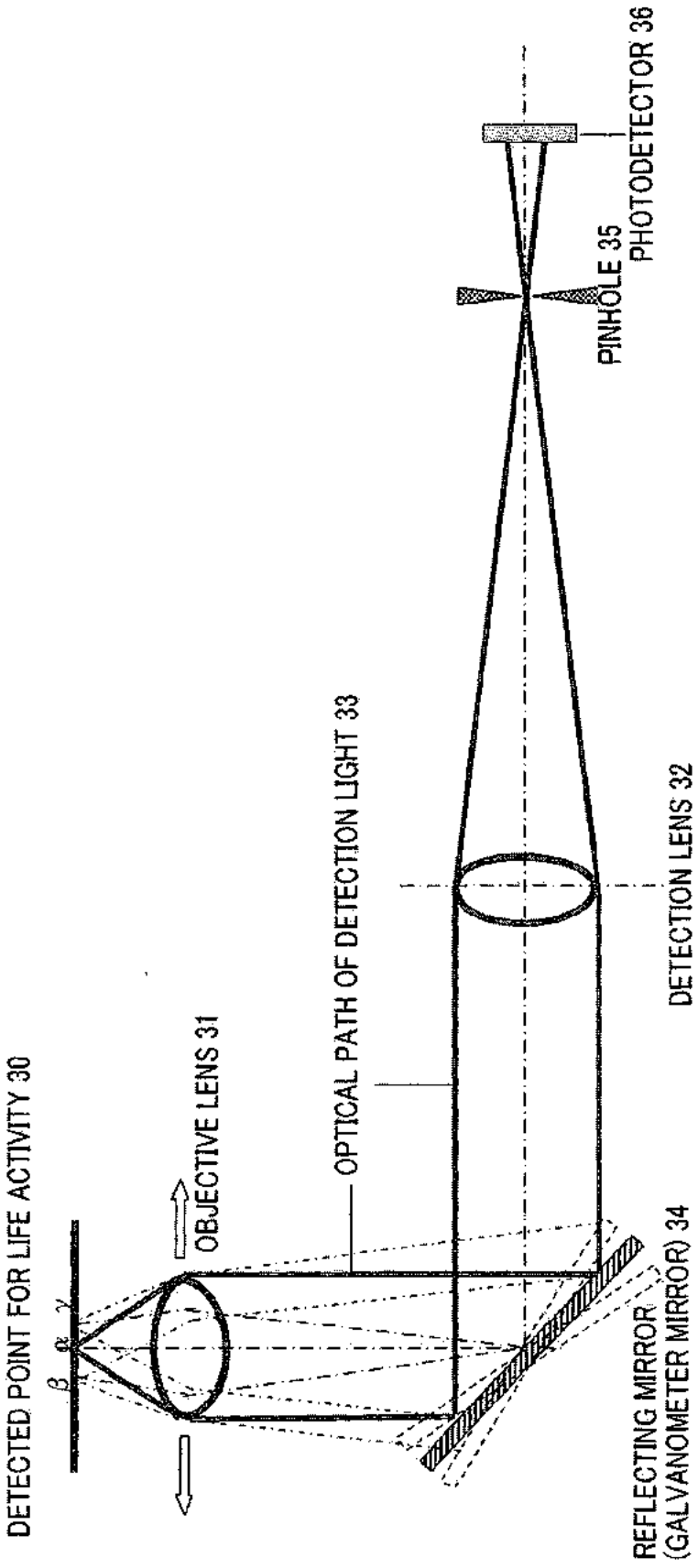



FIG.14 FIRST PRINCIPLE OF MONITORING METHOD OF DETECTED POINT FOR LIFE ACTIVITY

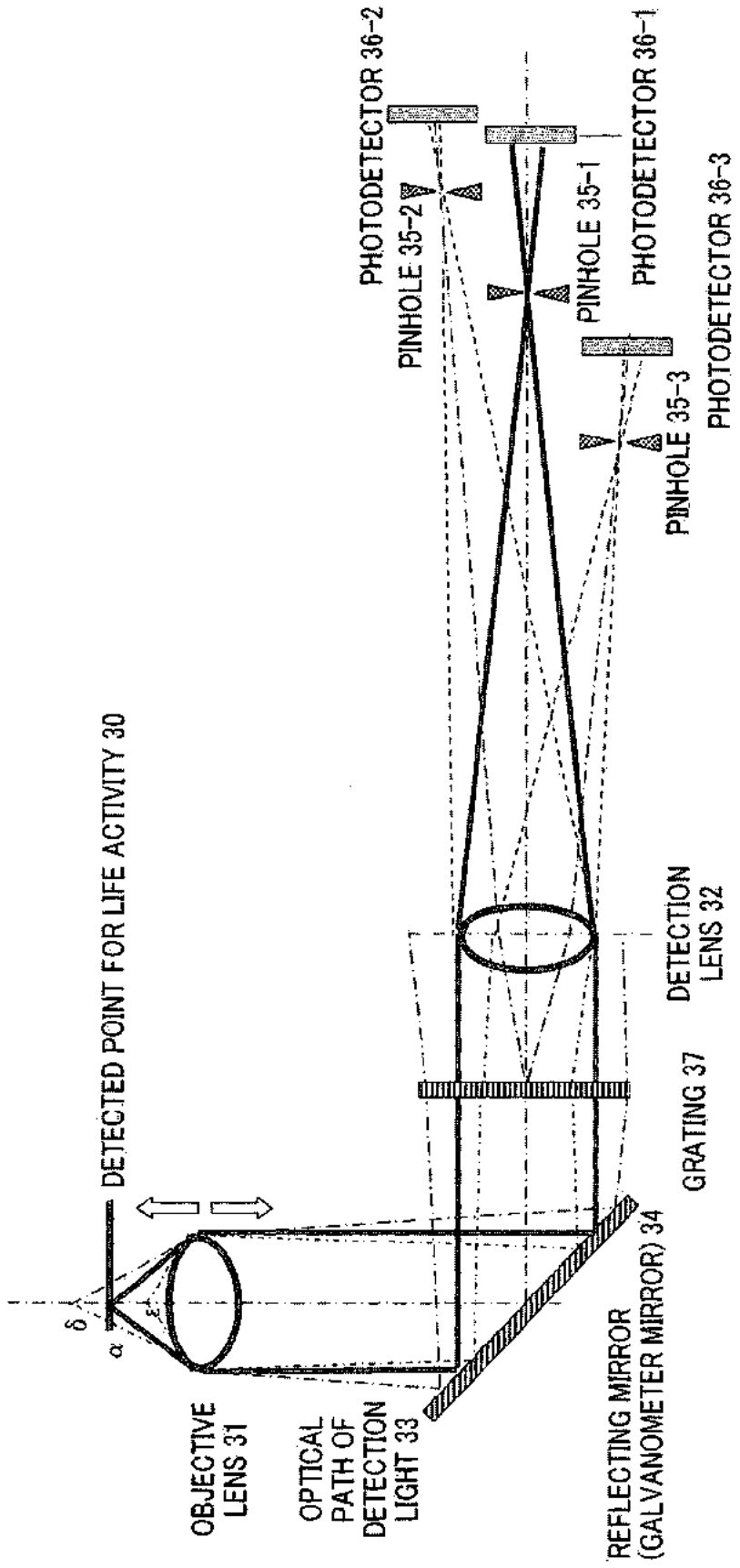



FIG.15 FIRST PRINCIPLE OF MONITORING METHOD OF PATTERN OF DETECTED POINT FOR LIFE ACTIVITY IN DEPTH DIRECTION

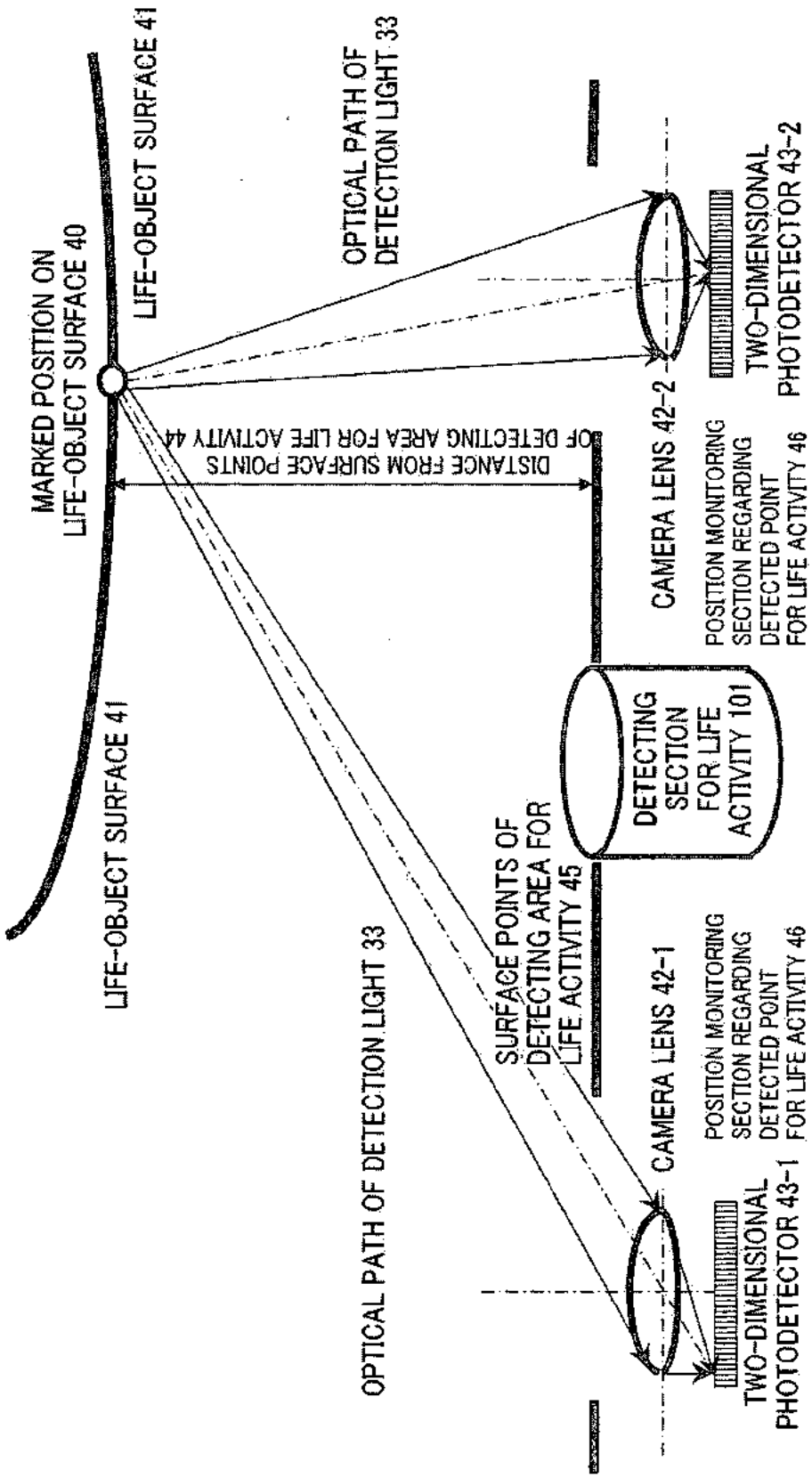



FIG.16 SECOND PRINCIPLE OF MONITORING METHOD OF MARKED POSITION ON LIFE-OBJECT SURFACE

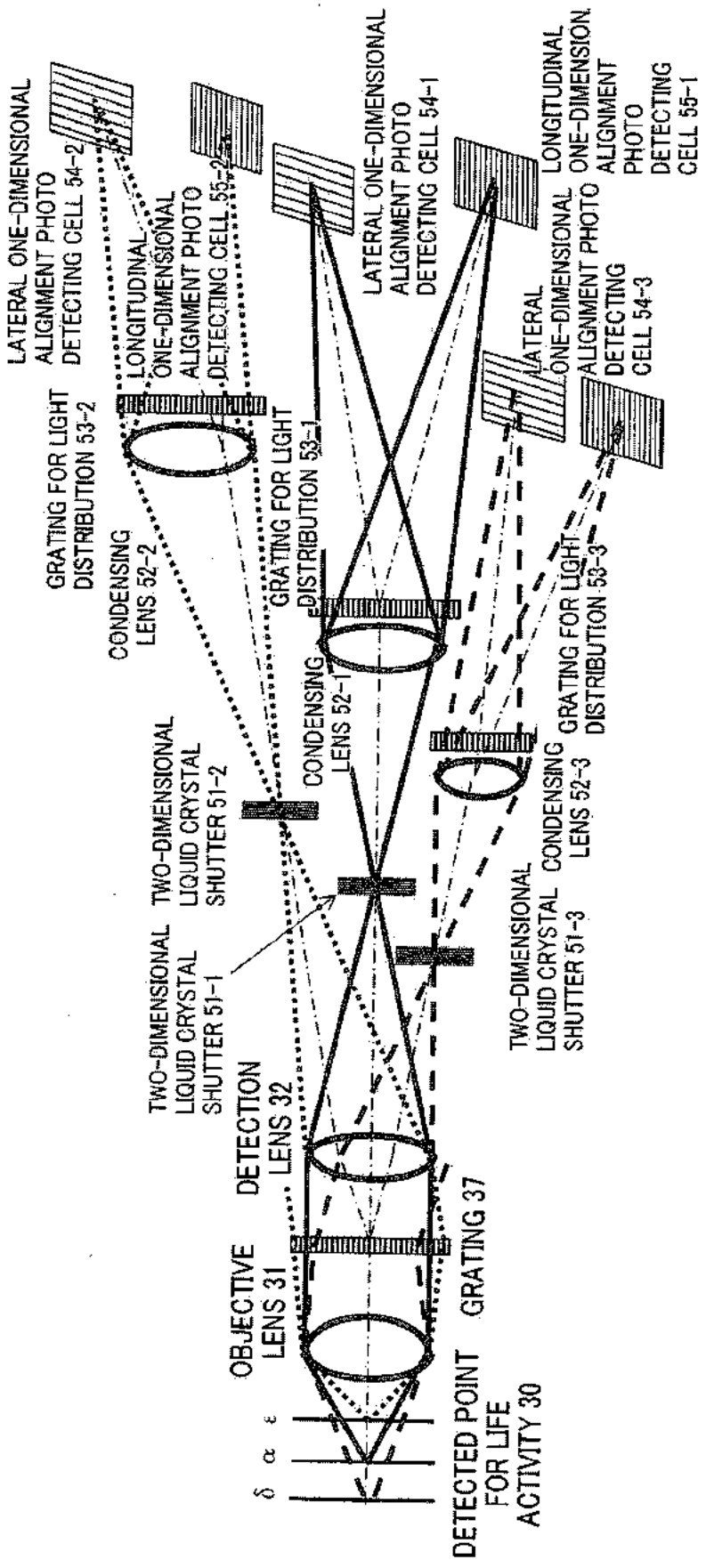



FIG.17 PRINCIPLE (USING CONFOCAL SYSTEM) OF FIRST EXEMPLARY EMBODIMENT REGARDING OPTICAL SYSTEM FOR LIFE ACTIVITY DETECTION

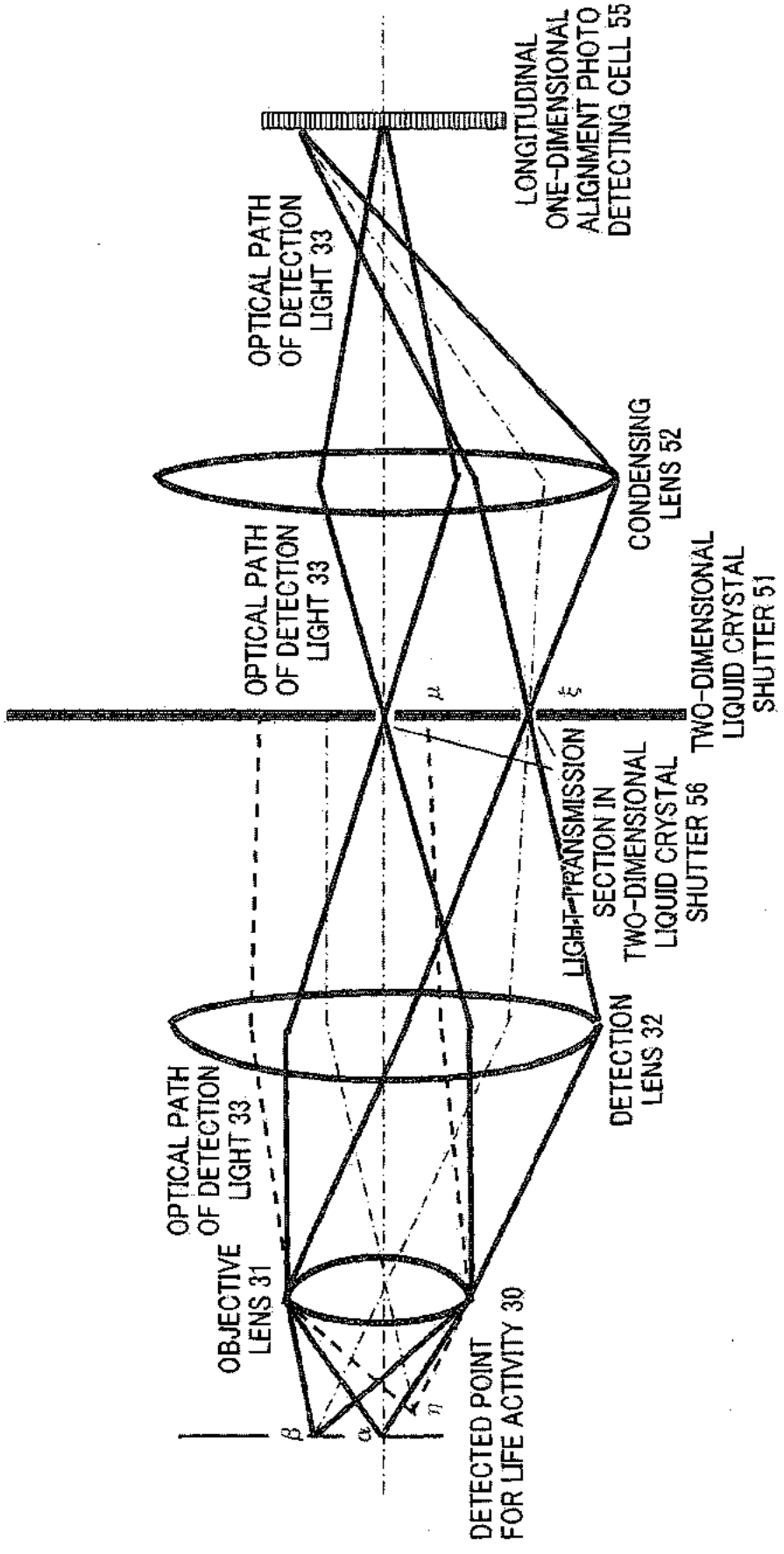
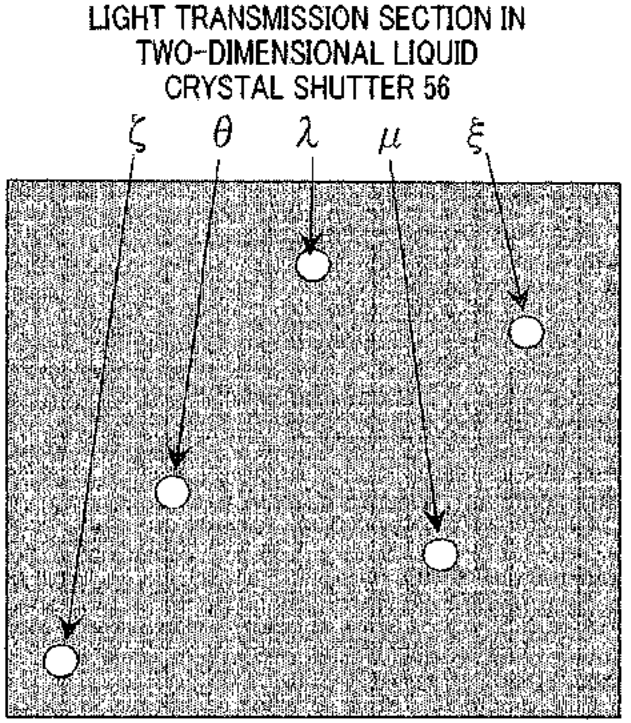
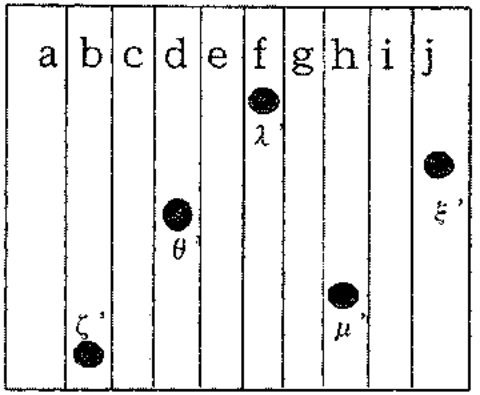


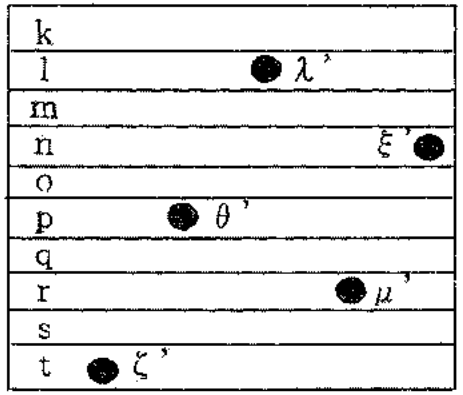

FIG.18 OPERATION PRINCIPLE OF FIRST EXEMPLARY EMBODIMENT REGARDING OPTICAL SYSTEM FOR LIFE ACTIVITY DETECTION




(a) PATTERN OF LIGHT TRANSMISSION SECTION IN TWO-DIMENSIONAL LIQUID CRYSTAL SHUTTER




(c) DETECTION LIGHT PATTERN OF LONGITUDINAL ONE-DIMENSIONAL ALIGNMENT PHOTO DETECTING CELL




(b) DETECTION LIGHT PATTERN OF LATERAL ONE-DIMENSIONAL ALIGNMENT PHOTO DETECTING CELL

FIG.19 RELATIONSHIP BETWEEN LIQUID CRYSTAL SHUTTER PATTERN AND PHOTO DETECTING CELL IN FIRST EXEMPLARY EMBODIMENT OF OPTICAL SYSTEM FOR LIFE ACTIVITY DETECTION

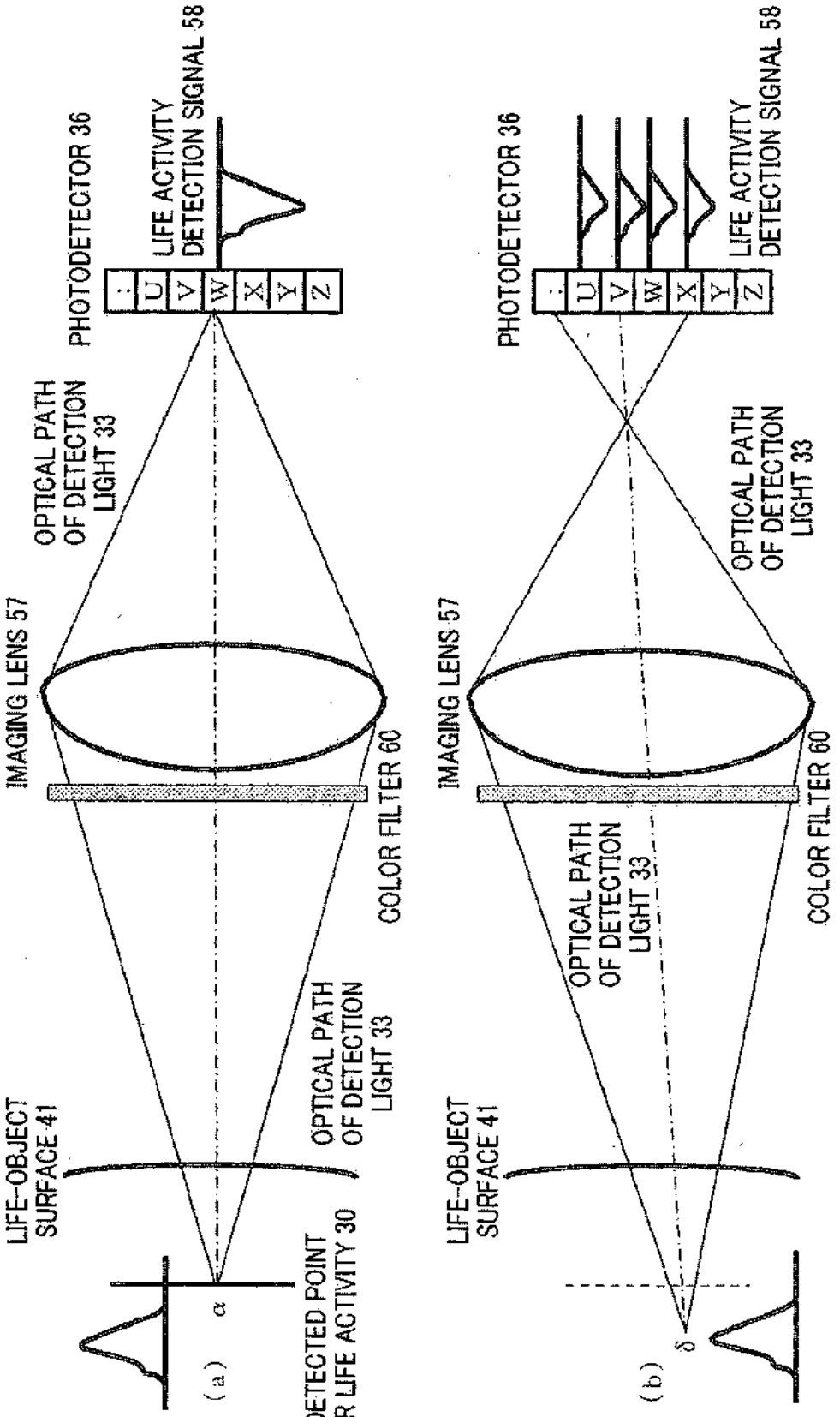



FIG.20 OPERATION PRINCIPLE REGARDING APPLIED EMBODIMENT OF OPTICAL SYSTEM FOR LIFE ACTIVITY DETECTION

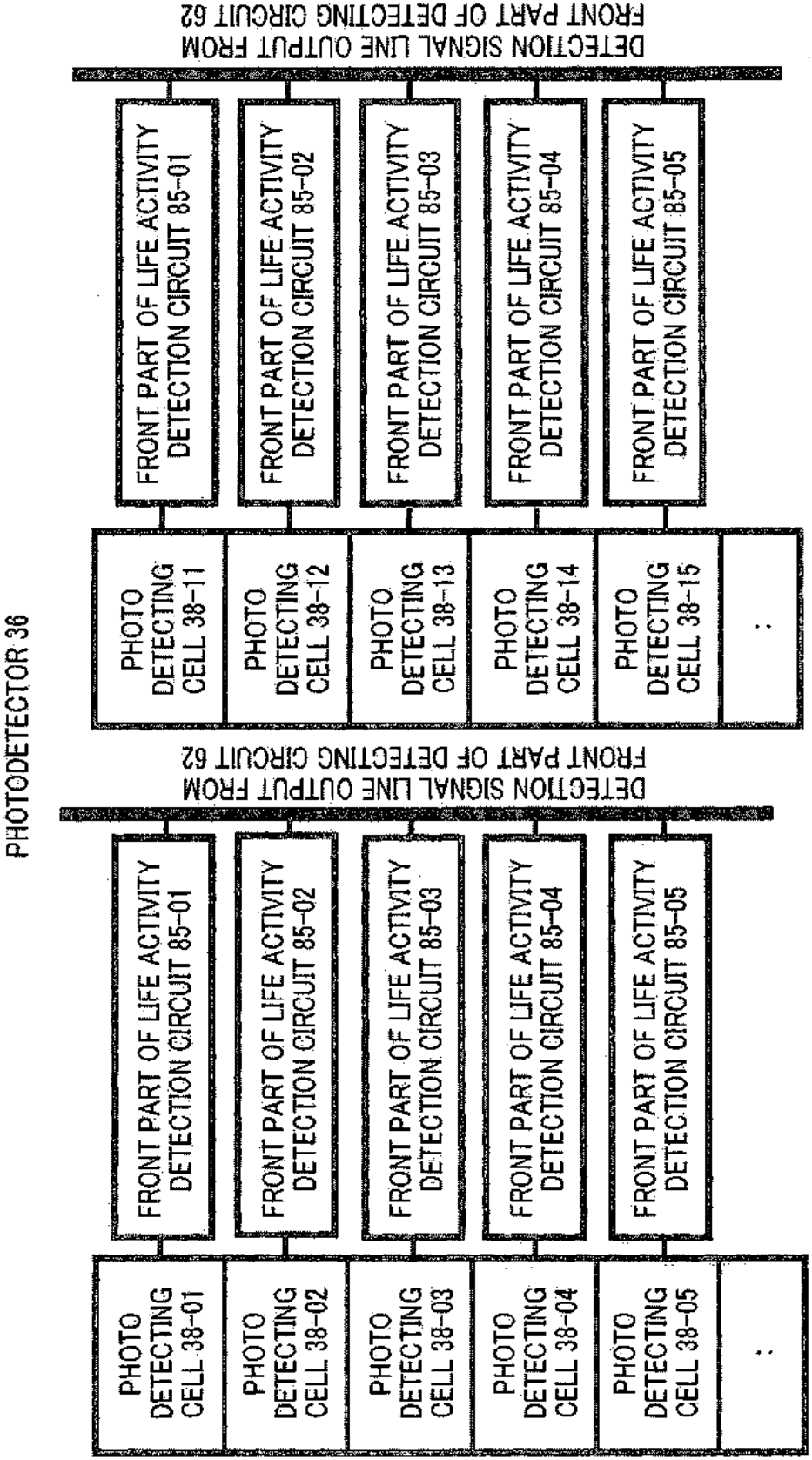



FIG.21 CONFIGURATION OF PHOTODETECTOR IN APPLIED EMBODIMENT OF OPTICAL SYSTEM FOR LIFE ACTIVITY DETECTION

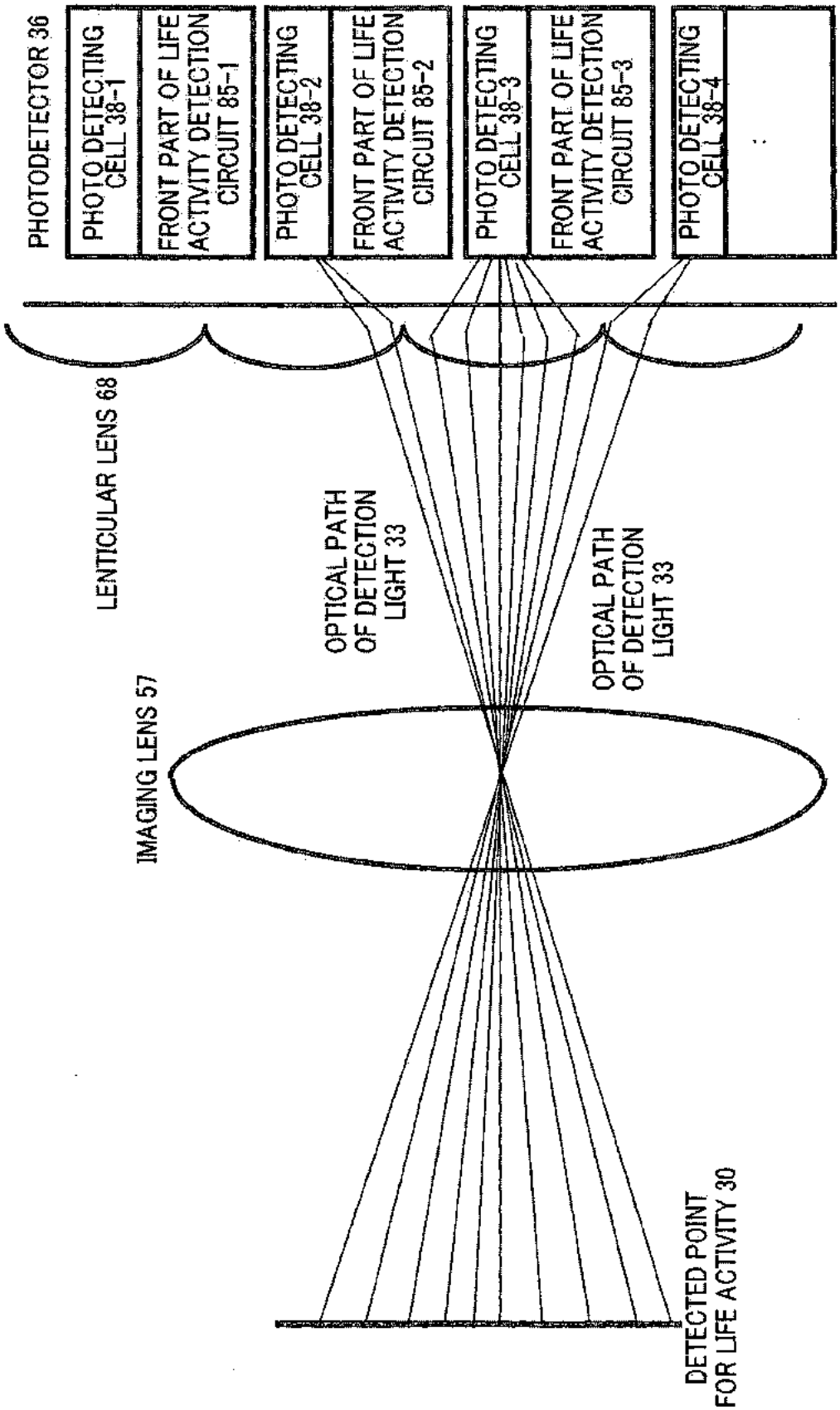



FIG.22 DETAILED OPTICAL ARRANGEMENT REGARDING APPLIED EMBODIMENT OF OPTICAL SYSTEM FOR LIFE ACTIVITY DETECTION

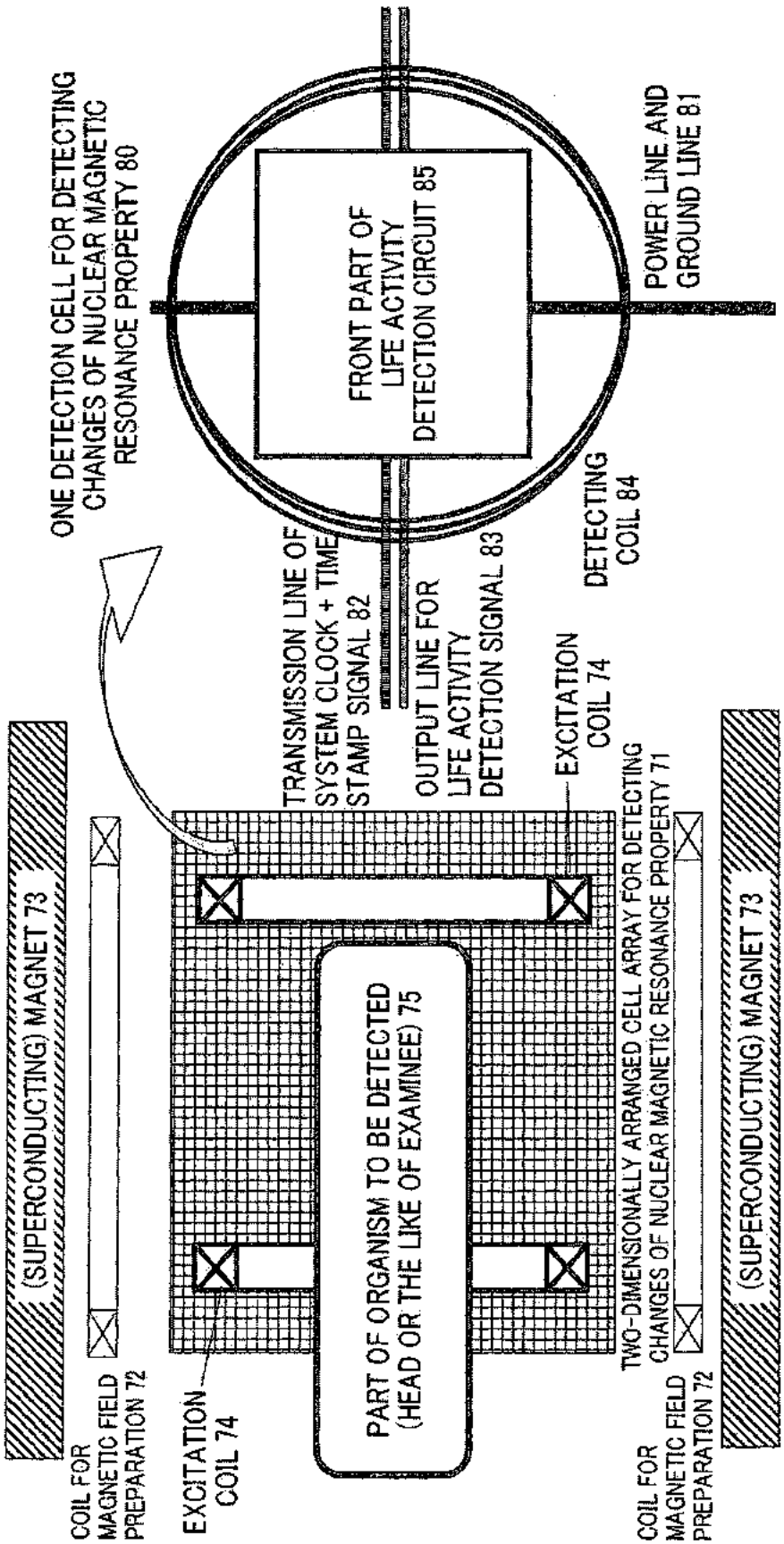



FIG.23 METHOD FOR DETECTING LOCAL CHANGE OF NUCLEAR MAGNETIC RESONANCE PROPERTY IN LIFE OBJECT AT HIGH SPEED

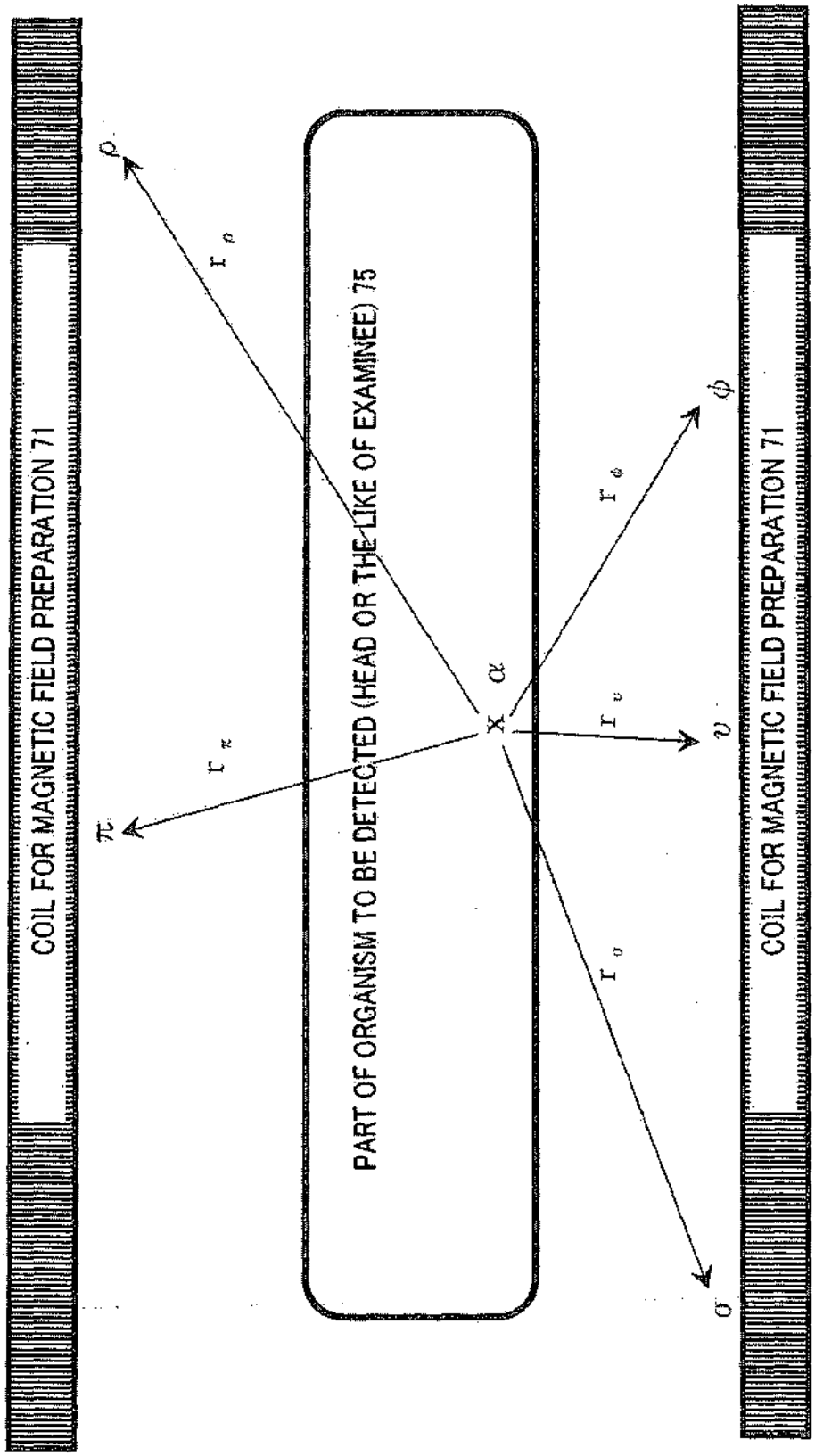
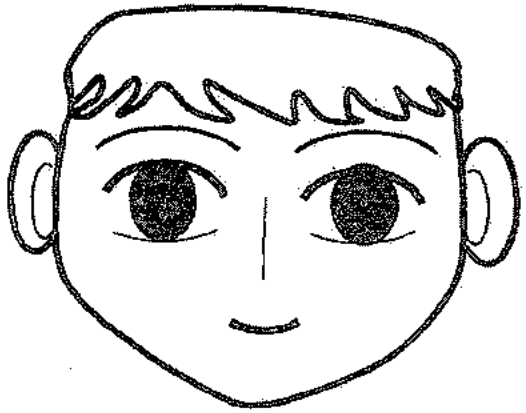
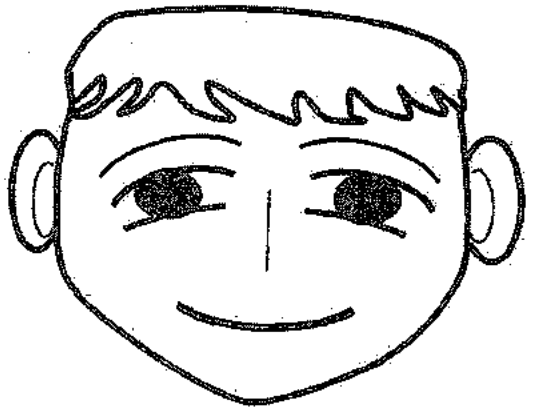


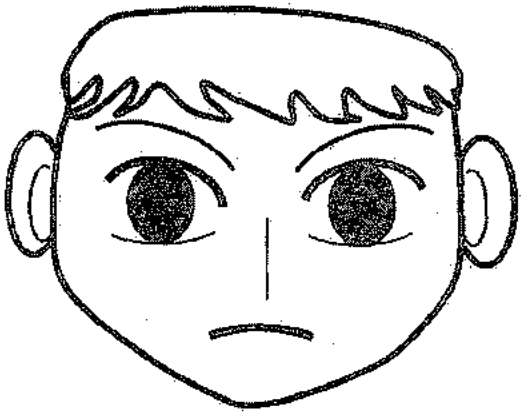

FIG.24 METHOD FOR DETECTING LOCATION WHERE NUCLEAR MAGNETIC RESONANCE PROPERTY CHANGES



(a) FACIAL EXPRESSION DURING REST



(b) FACIAL EXPRESSION AT THE TIME OF SMILING

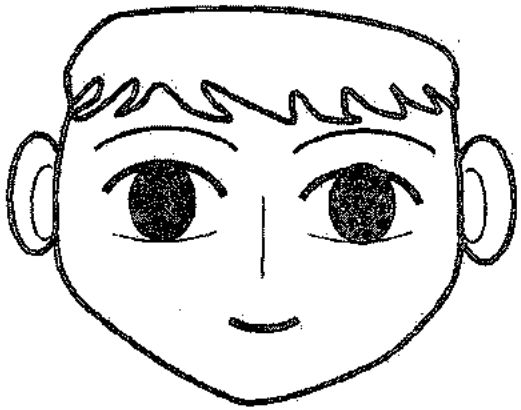


(c) FACIAL EXPRESSION AT THE TIME OF GETTING ANGRY

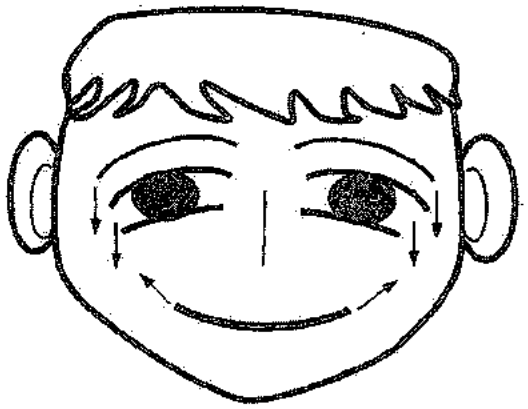


(d) FACIAL EXPRESSION AT A LOSS

FIG.25 RELATIONSHIP BETWEEN FACIAL EXPRESSION AND EMOTIONAL REACTION



(a) FACIAL EXPRESSION DURING REST



(b) FACIAL EXPRESSION AT THE TIME OF SMILING



(c) FACIAL EXPRESSION AT THE TIME OF GETTING ANGRY



(d) FACIAL EXPRESSION AT A LOSS

FIG.26 METHOD FOR OBTAINING LIFE ACTIVITY INFORMATION FROM MOVEMENT OF FACIAL MUSCLE

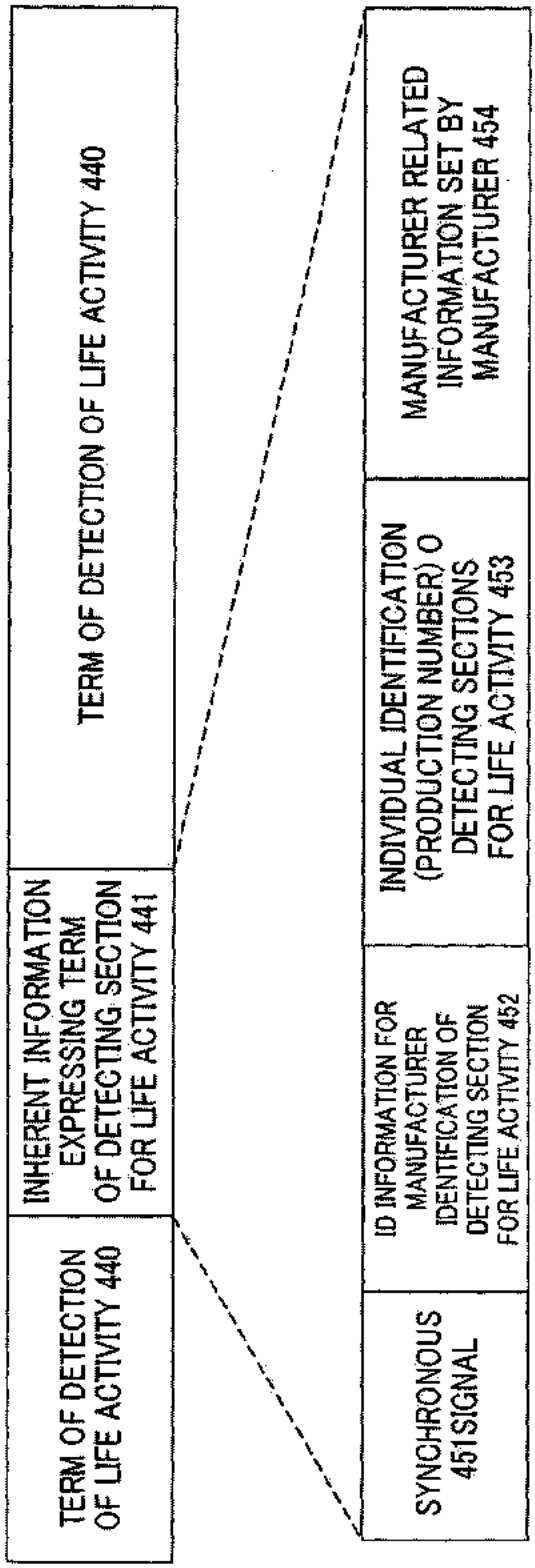



FIG.27 LIGHT EMITTING PATTERN OF ILLUMINATING LIGHT FOR LIFE ACTIVITY DETECTION IN DETECTION OF LIFE ACTIVITY

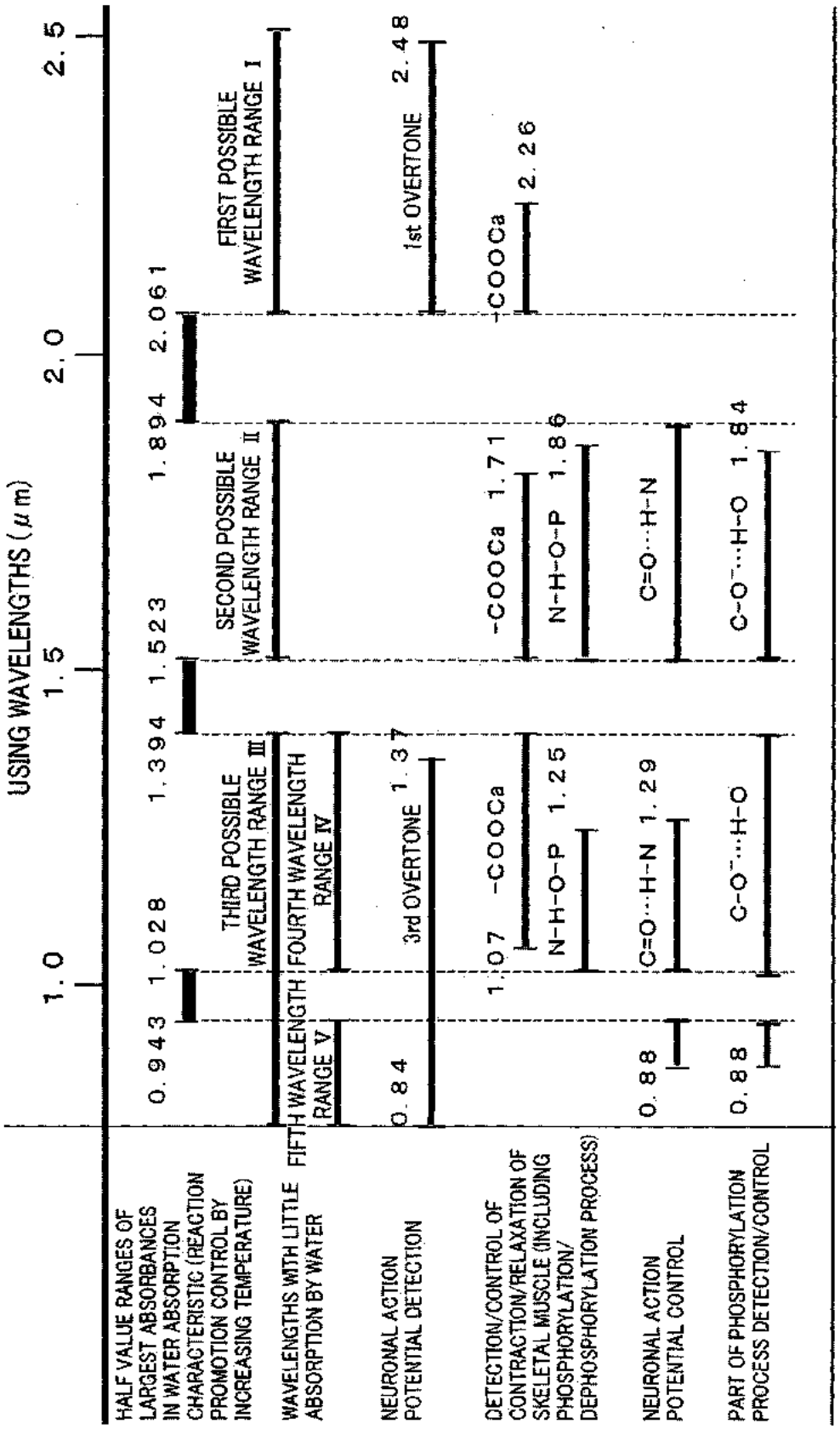



FIG.28 APPROPRIATE WAVELENGTHS FOR DETECTION/CONTROL OF LIFE ACTIVITY IN PRESENT EXEMPLARY EMBODIMENT/APPLIED EMBODIMENT

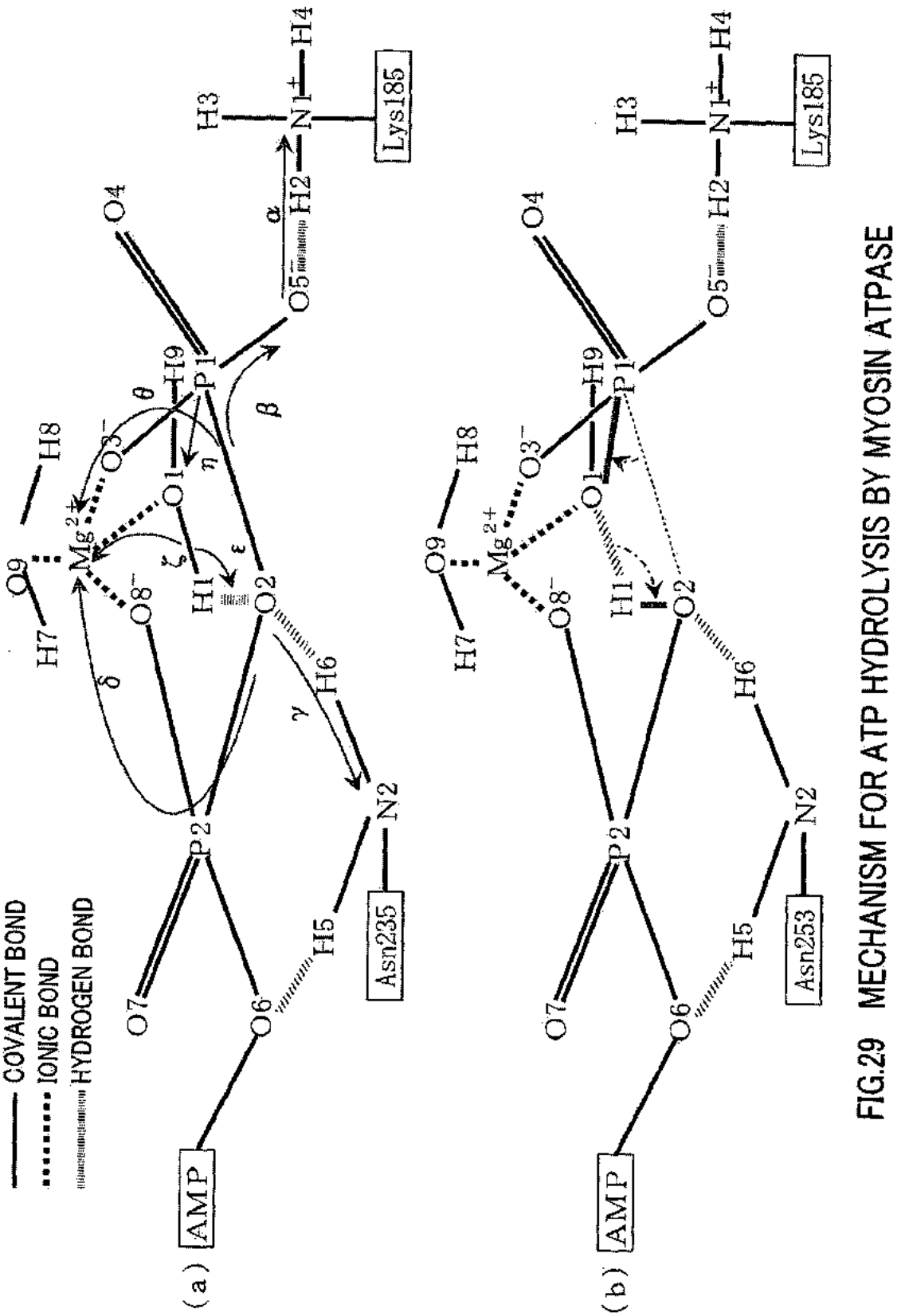



FIG.29 MECHANISM FOR ATP HYDROLYSIS BY MYOSIN ATPASE

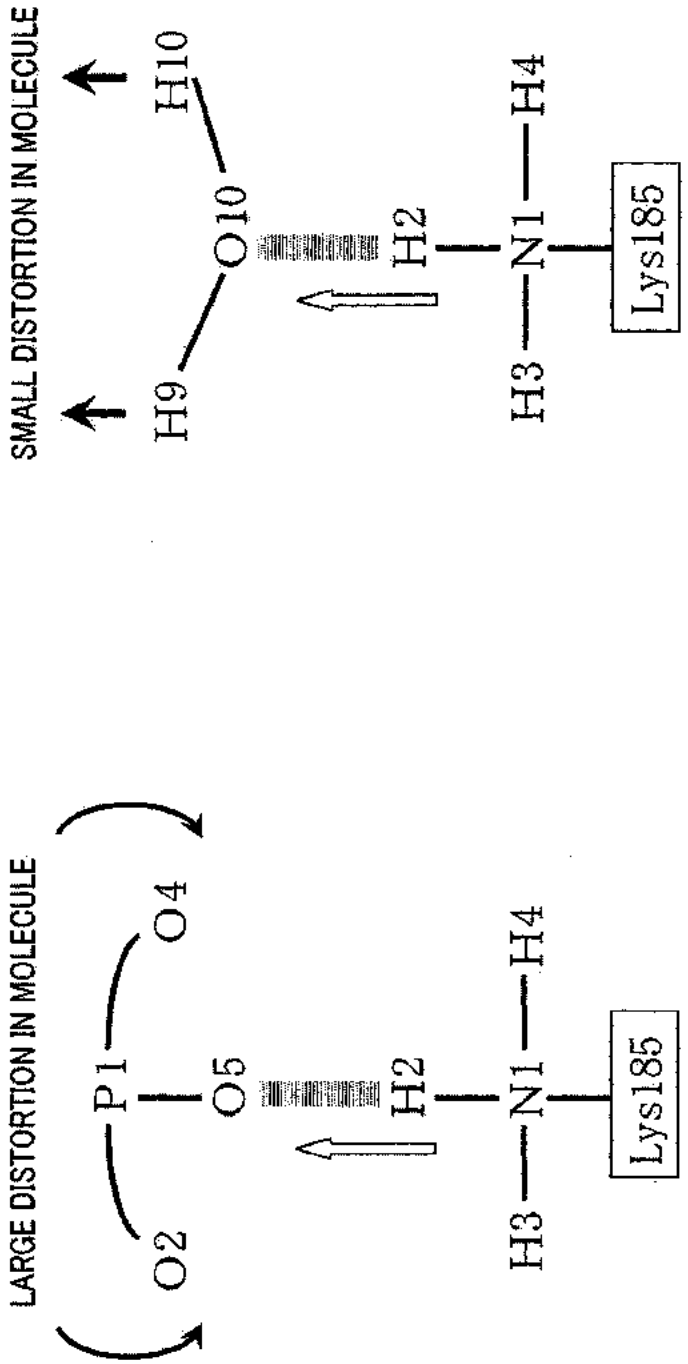



FIG.30 REASON WHY ABSORPTION BAND WAVELENGTH VARIES DEPENDING ON TO WHICH RESIDUE OF LYSINE IS HYDROGEN BONDED

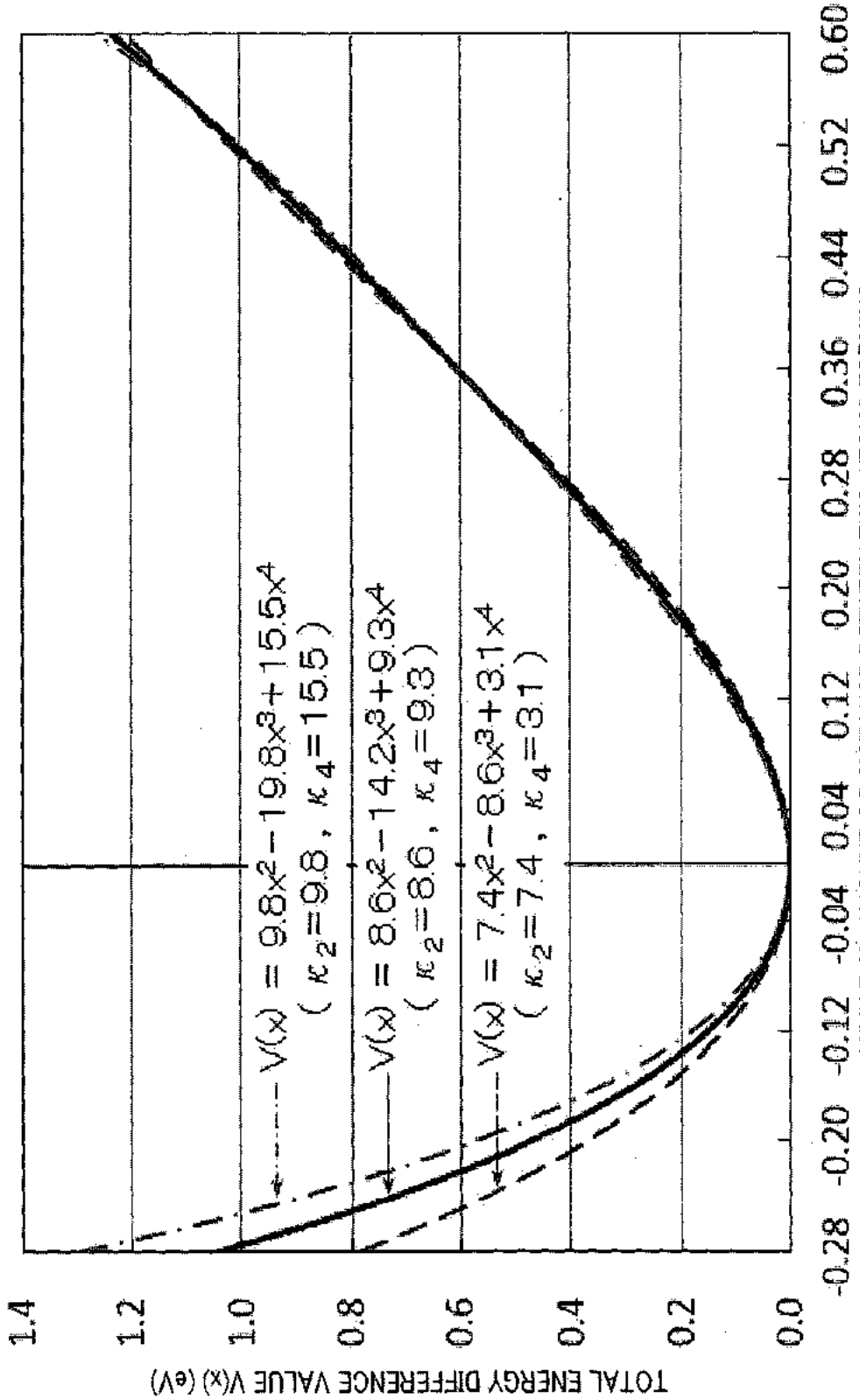



FIG.31 RELATIONSHIP BETWEEN HYDROGEN-BONDING PARTNER AND ANHARMONIC VIBRATION POTENTIAL PROPERTY

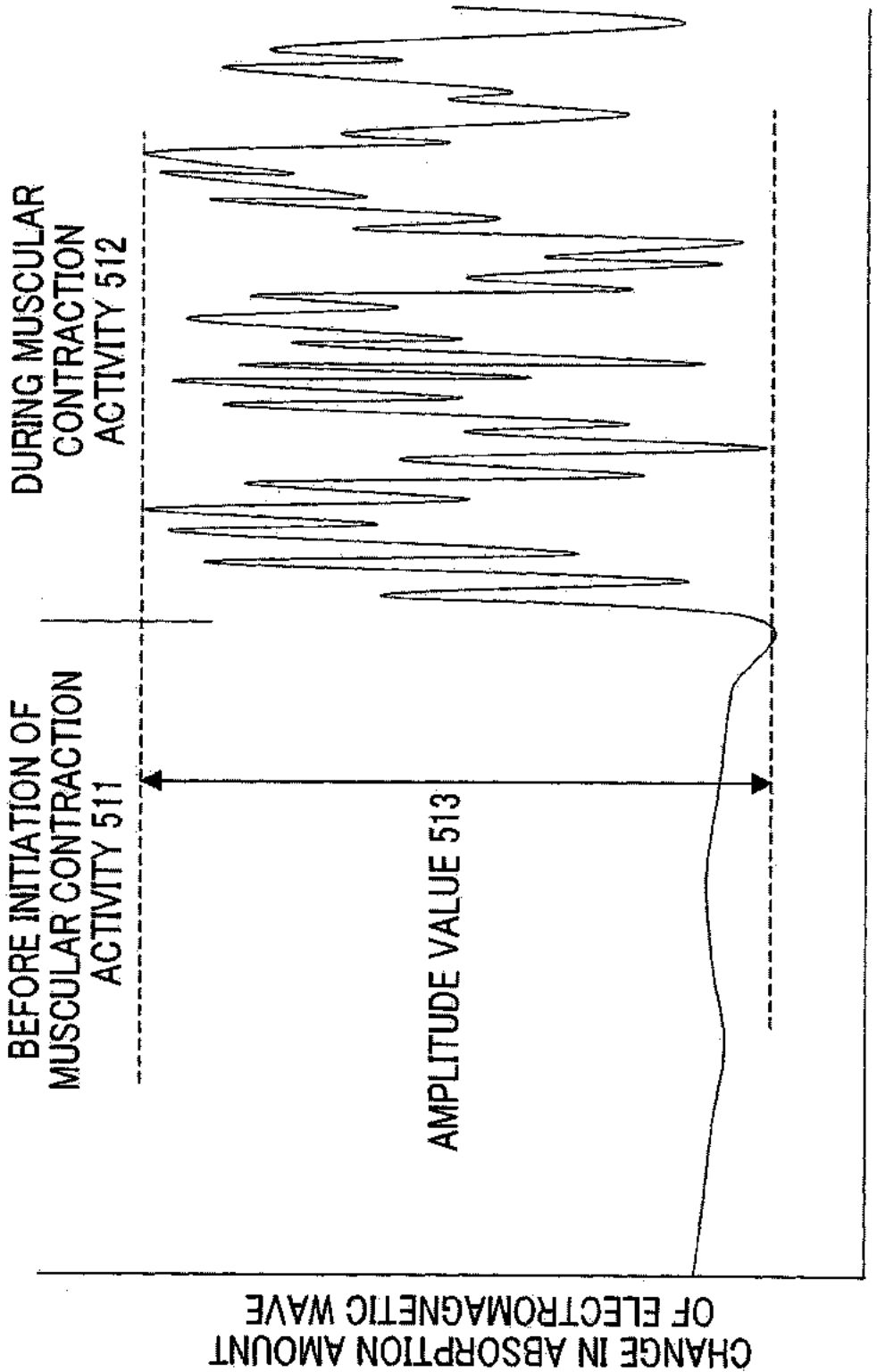



FIG.32 EXEMPLARY DETECTION SIGNAL RELATED TO MOVEMENT OF MIMETIC MUSCLE

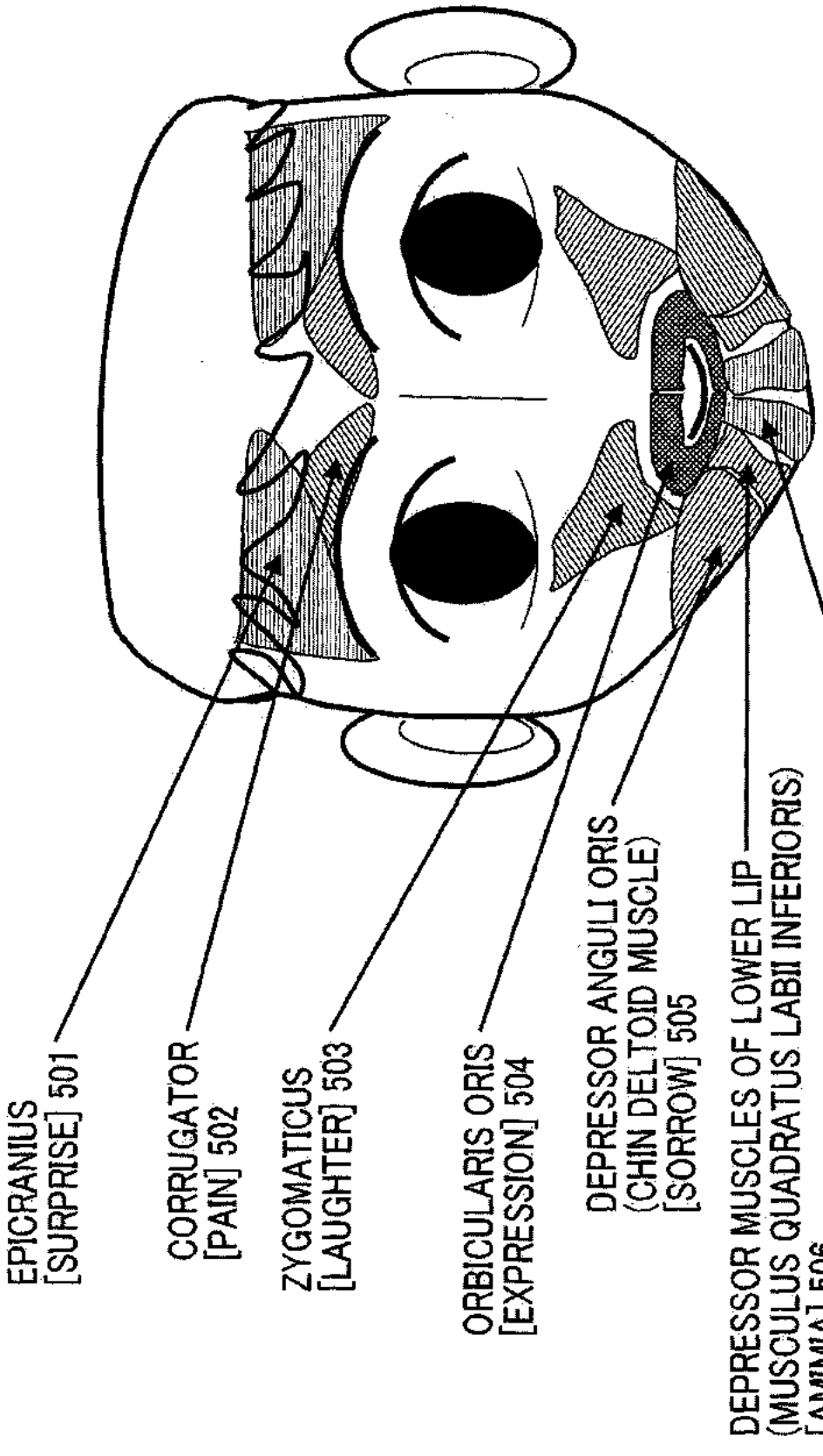



FIG.33 EXPLANATORY VIEW OF A RELATIONSHIP BETWEEN A LOCATION OF A MIMETIC MUSCLE WHICH CONTRACTS ON A FACE AND A FACIAL EXPRESSION

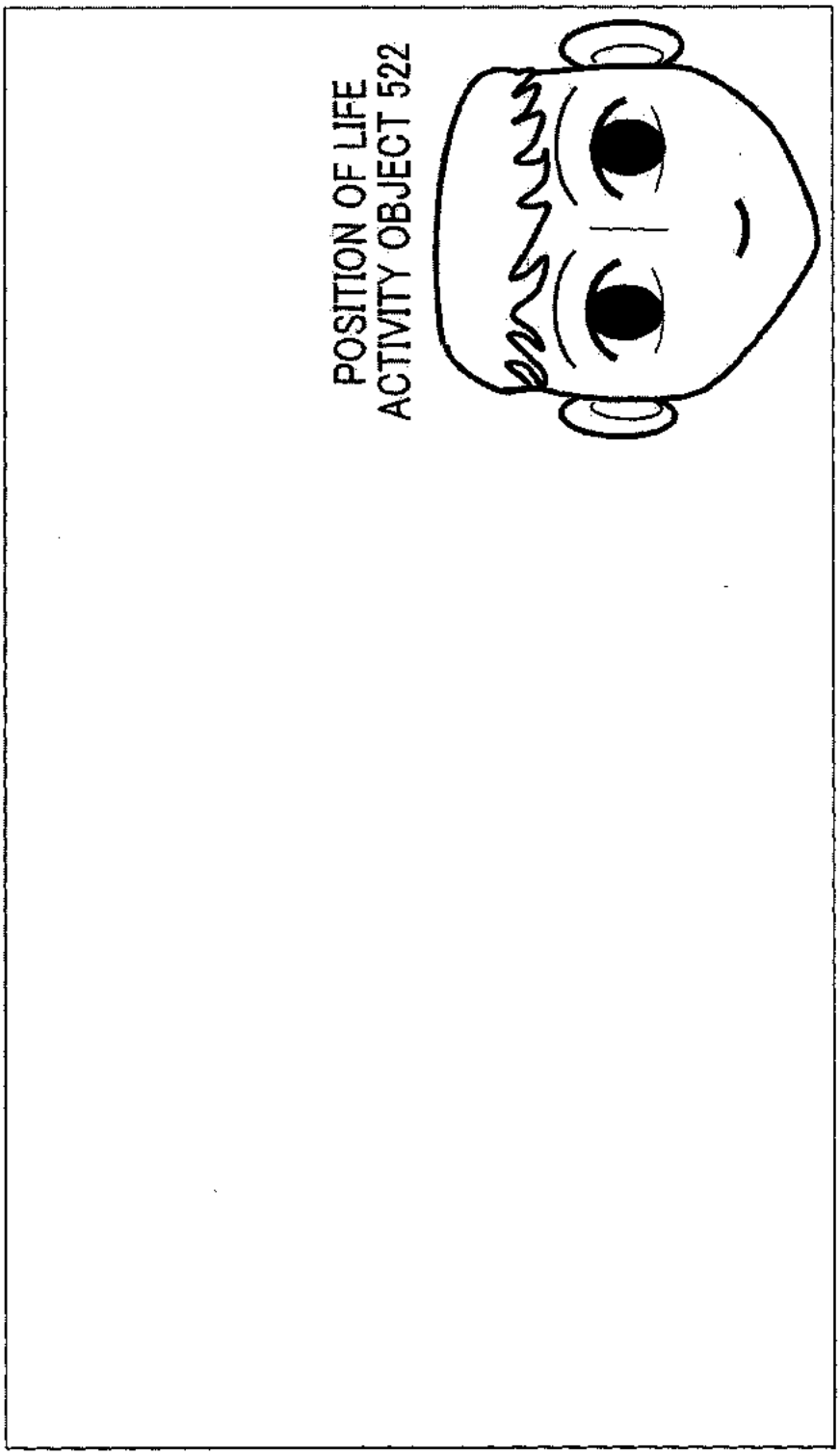



FIG.34 POSITIONAL RELATIONSHIP BETWEEN DETECTABLE RANGE AND DETECTION TARGET BY DETECTING SECTION FOR LIFE ACTIVIT

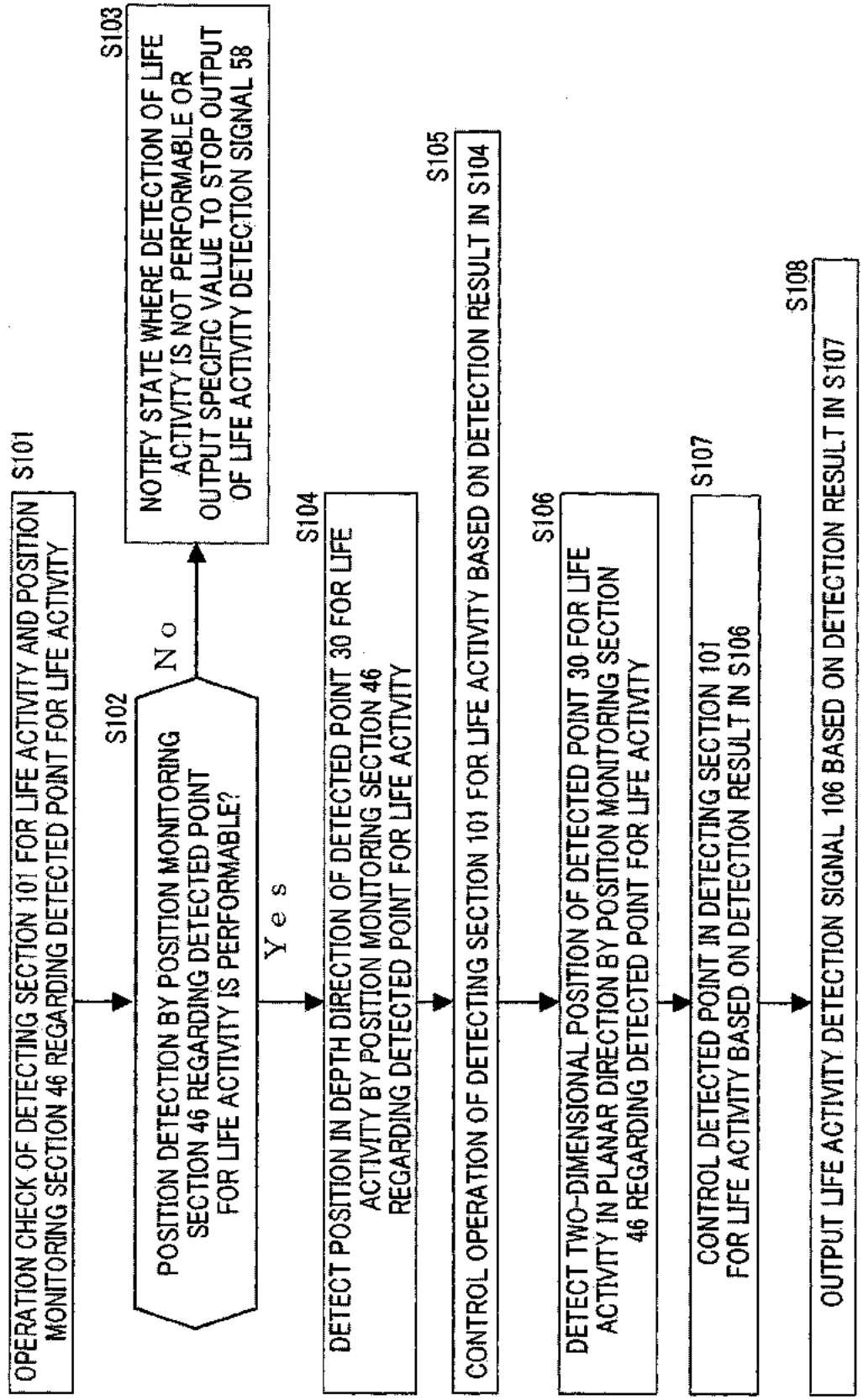



FIG.35 EXPLANATORY VIEW OF A MEASURING METHOD 1 OF LIFE ACTIVITY IN THE APPLIED EMBODIMENT

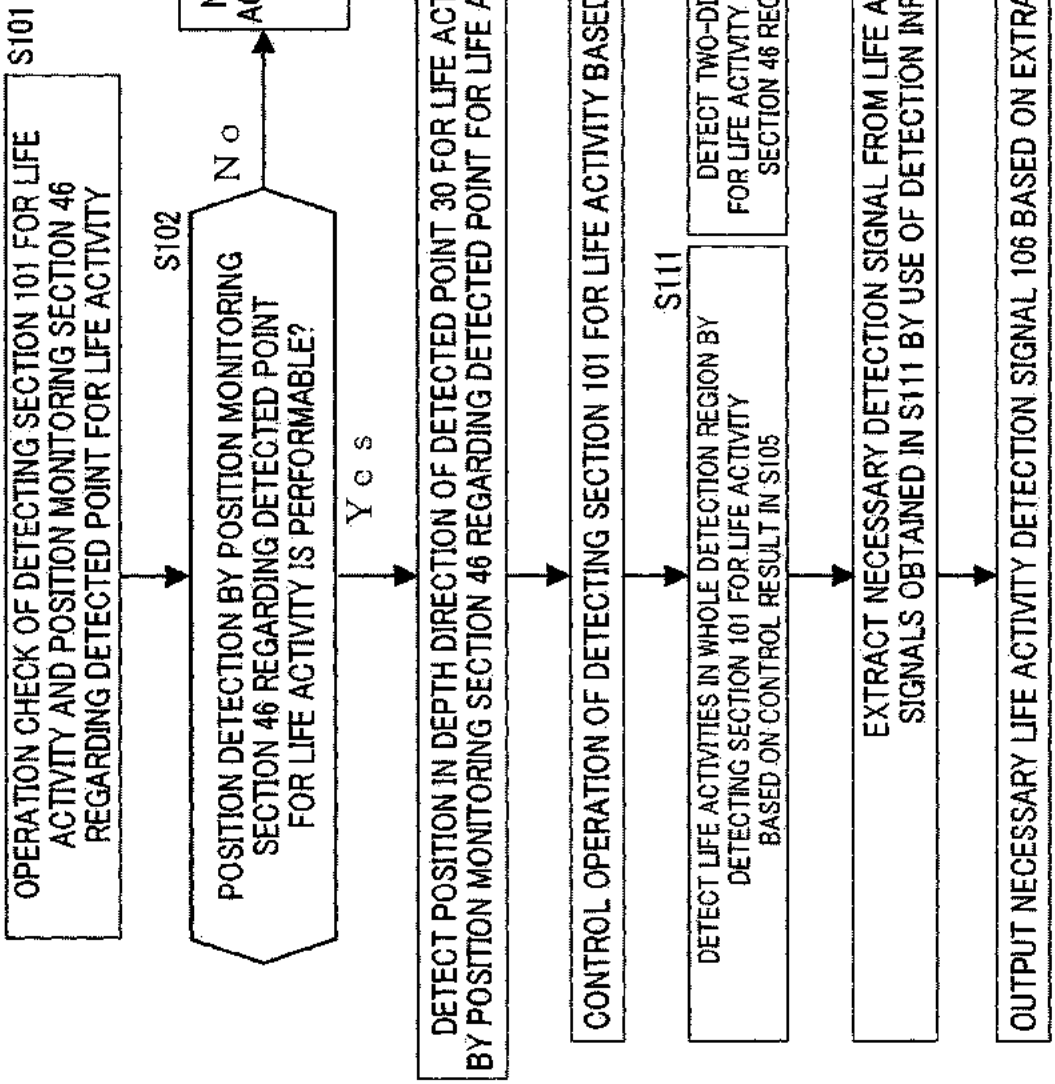



FIG.36 EXPLANATORY VIEW OF A MEASURING METHOD 2 OF LIFE ACTIVITY IN THE APPLIED EMBODIMENT

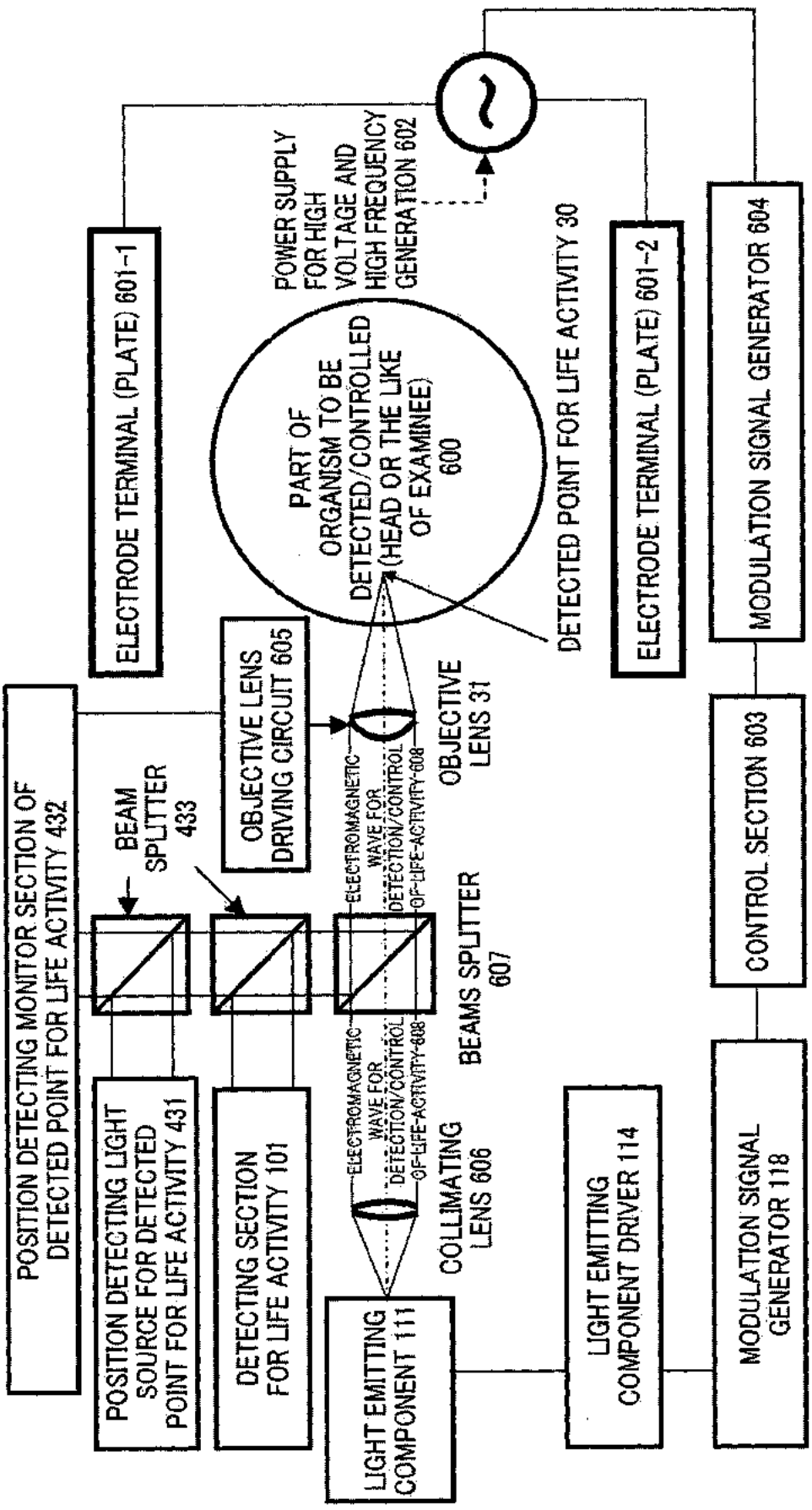



FIG.37 CONFIGURATION IN LIFE ACTIVITY CONTROL DEVICE IN PRESENT EXEMPLARY EMBODIMENT

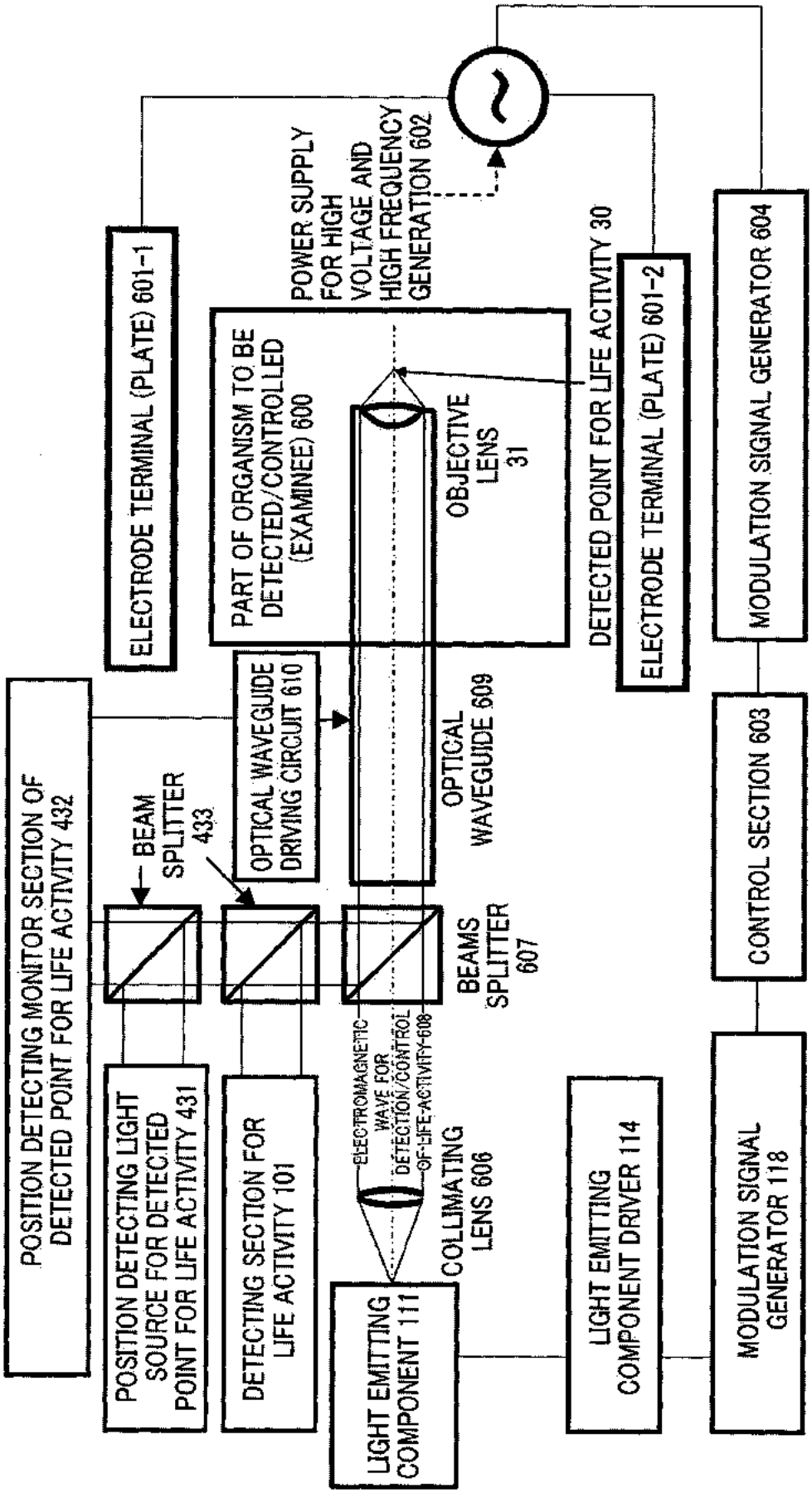



FIG.38 APPLIED EMBODIMENT OF LIFE ACTIVITY CONTROL DEVICE

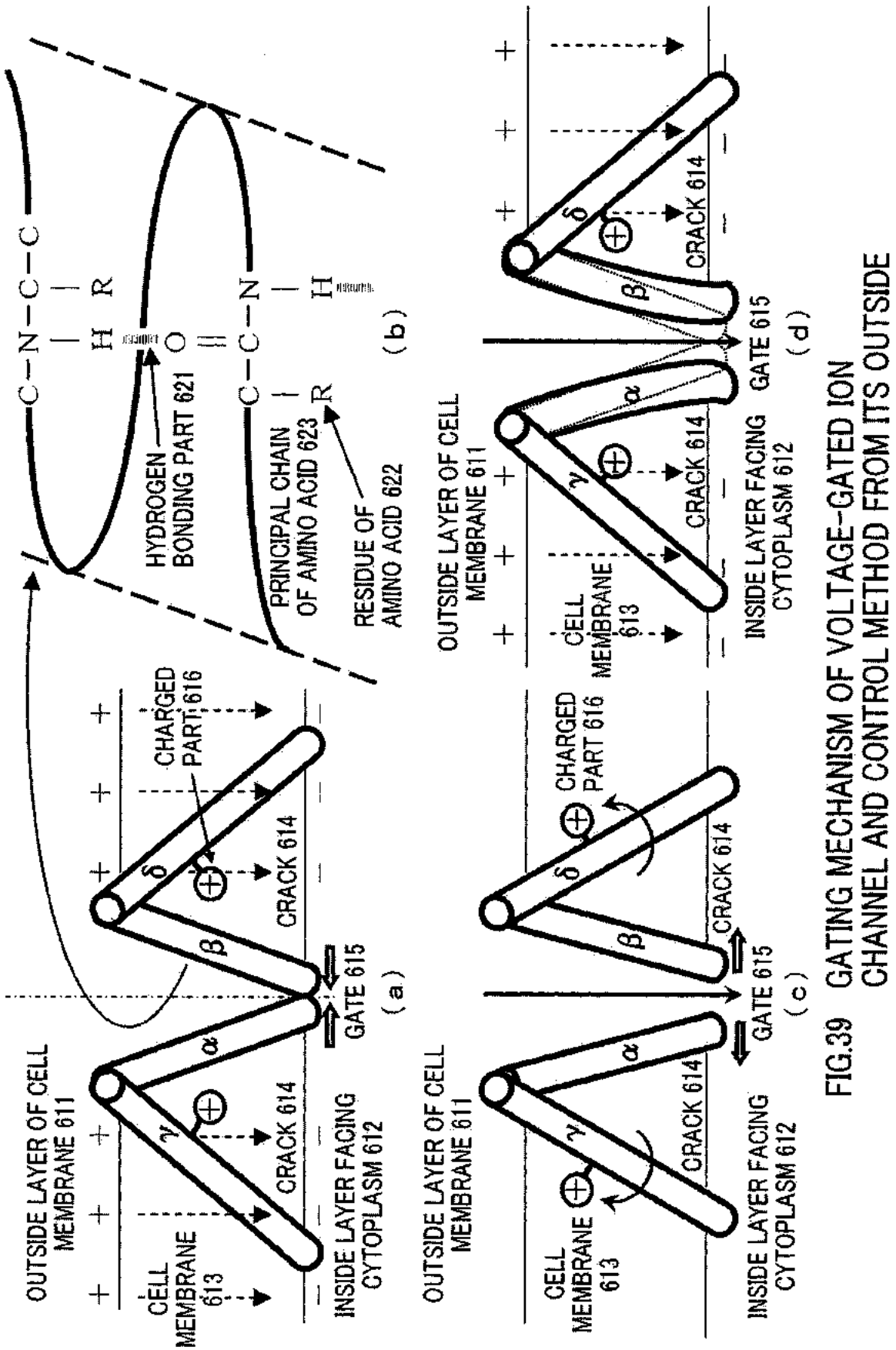



FIG.39 GATING MECHANISM OF VOLTAGE-GATED ION CHANNEL AND CONTROL METHOD FROM ITS OUTSIDE